UNIVERISTY OF OKLAHOMA

GRADUATE COLLEGE

MANGANESE TETRAOXIDE BASED POLYALKENOATE CEMENTS

A DISSERTATION

SUBMITTED TO THE GRADUATE FACULTY

in partial fulfillment of the requirements for the

degree of

Doctor of Philosophy

By

DIEGO A. ACOSTA
Norman, Oklahoma
2006

UMI Number: 3234987

ProQuest Information and Learning Company
300 North Zeeb Road
P.O. Box 1346
Ann Arbor, MI 48106-1346

MANGANESE TETRAOXIDE BASED POLYALKENOATE CEMENTS

A DISSERTATION APPROVED FOR THE
SCHOOL OF CHEMICAL, BIOLOGICAL ENGINEERING AND MATERIALS SCIENCE

BY

_____
Dr. Brian P. Grady (Chair)

_____
Dr. Jeffrey Harwell

_____
Dr. Dimitrios V. Papavassiliou

_____
Dr. Kenneth M. Nicholas

_____
Dr. Subhash N. Shah

To Lucia Restrepo de Acosta 1909-2004

ACKNOWLEDGMENTS

Many thanks to Dr. Brian P. Grady for being my advisor and on the path of earning my doctoral degree. Thanks also to my committee members: Dr. Jeffrey Harwell, Dr. Kenneth M. Nicholas, Dr. Dimitiros Papavassiliou, and Dr. Subhash Shah. Dr. Robert White from the chemistry department aided me with the FTIR measurements. XPS spectra were collected by Zhongrui Li. Thanks also to Alan Miles from the chemical engineering shop. This project was sponsored by Halliburton and thanks are also due to many people for their help and hospitality: Dr. Gary Funkhouser, Dr. Ian Robb, Dr. Wolfgang Deeg, Dr. Lewis Norman, Dr. Ron Lewis, and Rickey Morgan.

From the bottom of my heart I also want to acknowledge the following people: David Irwin, Gustavo Mesa, Gilberto Alvarez (rip), Hector J. Hoyos, Maria E. Sierra, Antonio Quintero, Javier Escobar, Luis F. Montoya, Edgar A. Mora, Gustavo Velasco, Javier Gutierrez, Juan E. Gomez, and Juan F. Londoño. Also, Norman was a good to me because of: Jose F. Alvarez, Maricel Marquez, Russ Merchant, Dr. Hatice Gecol, and Dr. Andrew Carswell.

My family provides me with love, encouragement, and support. This Ph.D. belongs to: Luz Amparo Maya de Acosta, Jose Ignacio Acosta, Santiago Acosta, Lina Villa de Acosta, my soon to be born nephew Pedro Acosta, and the furry members of the family: Tobias, Candelario, Congo, Roque and Omar David.

CONTENTS

TABLES

ILLUSTRATIONS

PREFACE

Portland cement has been used in different applications like oil-well cementing. Economic considerations as well as physical properties are supremely important in oil-well cementing and coming up with an alternative for Portland cement implies that it has to surpass it both in cost and performance. Polyalkenoate cements provides a chemistry that should result in a material capable of outperforming Portland cement; although at a higher cost. Standard polyalkenoate cements use a preformed polymer acid such as poly(acrylic acid) and acid-degradable glass. The latter both releases multivalent cations and serves to stiffen the cement. Acid-degradable glass is too expensive for large-scale industrial applications, and the use of a preformed polymer is unacceptable for large-scale transfer of the material. Because of these drawbacks, a new polyalkenoate cement was devised.

There are several fillers and polyalkenoic acids that could be used to design new polyalkenoates. Intense experimentation was done to find suitable compositions that would result in hardened polyalkenoate cement. Through design of experiments it was found that some of the independent variables, such as acrylic acid/initiator mol ratio, had no impact on the mechanical properties and rheology of the polyalkenoate cement and slurries, while others, like acrylic acid/cation mol ratio, proved to be relevant. The purpose of this research shows how we devised a novel polyalkenoate cement, modeled its mechanical properties and rheology, and characterized the cement on a molecular level in order to understand why specific formulations led to the observed performance.

CHAPTER 1

INTRODUCTION

Composite Materials

A composite is a material made of filler particles surrounded by a matrix of a second material that binds the filler particles together. In many composites, the purpose of the filler is to impart the composite with improved mechanical properties. In order for this improvement to occur, external stresses are transferred from the continuous phase to the discontinuous phase (filler). Due to the wide variety of matrix and filler materials available, there is a vast potential for research in this area and the design of novel materials.

Composite materials are further sub classified according to the morphology and size of the filler as fibrous composites, particulate composites, nanocomposites, etc. Commercial composites generally employ a polymer matrix like polyester, polyvinyl, epoxy resins, phenolic resins, polyimide, polyamide, etc. as the continuous phase. The fillers include a variety of materials capable of binding with the continuous phase. The disposition of the filler in this binding matrix can be random or oriented. Examples of composite materials include fiber-reinforced plastics, ceramic matrix composites like Portland cement, organic matrix/ceramic aggregate composites like dental cements, engineered wood like ply-wood, etc. Natural composite materials examples include bones and wood.

Cements

One of the most important composites is cement. This material has a number of uses and many of them result from their ability to bond to other materials. Despite being a common material, the term cement is defined in two ways: cement can be considered a paste that is prepared by mixing a powder and water that sets into a hard mass. Other definition considers cement as a bonding agent. While both definitions are correct, they pertain to different things, which are the setting process of cement and a physical property. In concrete, cement is the continuous phase and gravel is the filler, while in oil-well cementing hydraulic cement is a paste that sets into a hard mass[1]. Both definitions are pertinent in this project because in some formulations flyash is used in an analogous manner as gravel is used in concrete. Other formulations employing hausmannite, acrylic acid, initiator and water can well be considered a paste that sets into a hard mass by itself.

Cements are classified into hydraulic cements, condensation cements and acid-base cements[2]. Hydraulic cements are commonly utilized in a number of different industries including structural (e.g., in the construction of buildings and roads), and energy (e.g., subterranean well completion and remedial operations.) The primary components of a typical hydraulic cement include Portland cement, water, rock, and sand. In hydraulic cements, setting occurs by a hydration-precipitation process[1]. The undesirable attributes of this material include its poor flexibility, low tensile strength and the inability to effectively control hardening time.

Condensation cements formation occurs through a loss of water and condensation of two hydroxyl groups to form a bridging oxygen:

$$R-OH+OH-R \rightarrow R-O-R+H_2O$$

Examples of these cements include silicate cement where orthosilicic acid condenses to form a silicic acid gel, and refractory cements formed by heat treatment of acid orthophosphate to form a polyphosphate. These cements have many of the same drawbacks as hydraulic cements.

Acid-base cements are cementitious salt hydrogels resulting from the reaction between a basic metal oxide and an acid via an acid-base reaction. Because the acid-base cements are quick setting and have unusual properties for cements such as adhesion and improved mechanical properties, they find numerous applications in dentistry and industry[2].

Polyalkenoate cements are a subset of acid-base cements; where the acid is a polymer that contains acid groups, and the base contains a multivalent cation and need not be a metal oxide. Because of these properties, polyalkenoate cements were investigated as a replacement for Portland cement in one specific application, namely oil-well cementing. The next two sections describe in detail the chemistry of Portland cement and polyalkenoate cements.

Portland Cements

Portland cement is the most common hydraulic cement. Different types of Portland cement are manufactured to meet different physical and chemical requirements for specific purposes, such as durability and high-early strength. Cement chemistry is very complex, so a notation (shown in Table 1) was invented to simplify the formula of common components found in cement[1].

Table 1. Cement chemistry notation of typical cement components

Cement Chemistry Notation	*Chemical Formula*
C	CaO
S	SiO_2
A	Al_2O_3
F	Fe_2O_3
T	TiO_2
M	MgO
K	K_2O
N	Na_2O
H	H_2O
C_3S	$3CaO{\cdot}SiO_2$
$\bar{C}$	CO_3
$\bar{S}$	SO_3
C_2S	$2CaO{\cdot}SiO_2$
C_3A	$3CaO{\cdot}Al_2O_3$
C_4AF	$4CaO{\cdot}Al_2O_3{\cdot}Fe_2O_3$
Aft	$[Ca_3Al(OH)_6{\cdot}12H_2O]_2{\cdot}(SO_4)3{\cdot}2H_2O$
Afm	$3CaO{\cdot}Al_2O_3{\cdot}CaSO_4{\cdot}12H_2O$

The phase compositions in Portland cement are denoted as tricalcium silicate (C3S), dicalcium silicate (C2S), tricalcium aluminate (C3A), and tetracalcium aluminoferrite (C4AF). It should be noted that these compositions would occur at phase equilibrium of all components in the mix and do not reflect effects of processing conditions such as temperature, oxygen availability, and other kiln conditions. The components for Portland cement production are a mixture of calcium oxide, silicon oxide, aluminium oxide, ferric oxide, and magnesium oxide. These materials are usually mined locally in some places where the desired components are already availablewhile in other places the addition of clay and limestone, as well as iron ore, bauxite or recycled materials is needed. The low

cost and widespread availability of limestone, shales, and other natural materials make Portland cement one of the most economic materials. This mixture is heated in a rotary kiln, which is a sloped cylinder, with temperatures increasing over the length of the cylinder up to 1500°C. The temperature is regulated so that the product contains sintered but not fused lumps. A temperature that is too low causes insufficient sintering, while a temperature that is too high results in a molten mass or glass. In the lower-temperature region of the kiln, calcium carbonate (limestone) turns into calcium oxide (lime) and carbon dioxide. In the high-temperature part, calcium oxides and silicates react to form dicalcium and tricalcium silicates (C2S and C3S). Small amounts of tricalcium aluminate (C3A) and tetracalcium aluminoferrite (C4AF) are also formed.

The resulting material or clinker consists of particulate material with mean sizes ranging between 1 mm and 25 mm, which can be stored before use. Prolonged exposure to water however, decreases the reactivity of cement produced from weathered clinker. In order to achieve the desired setting qualities in the finished product, about 2% of gypsum is added to the clinker and then the mixture is finely pulverized. This cement powder is now ready for use, and will react with water. When water is mixed with Portland cement, the product sets in a few hours and hardens over time. The initial setting is caused by a reaction between the water, gypsum, and tricalcium aluminate (C3A), forming the crystalline hydration products calcium-alumino-hydrate (CAH), ettringite (Aft), and monosulfate (Afm) (see Table 1)

Later hardening and development of cohesive strength is due to the reaction of water and tricalcium silicate (C3S), forming an amorphous hydrated product called calcium-silicate-hydrate (CSH gel). In each case the hydration products surround and cement together the individual grains. The hydration of dicalcium silicate (C2S) proceeds more

slowly than that of the above compounds slowly increasing strength. All three reactions mentioned above are exothermic.

Table 2. Types of Portland cements

Type	***Typical composition % (wt.)***							***ASTM description***
	C_3S	***C_2S***	***C_3A***	***C_4AF***	***M***	***SO_3***	***C***	
I	55	19	10	7	2.8	2.9	1	General purpose cement; $C_3A<15\%$
II	51	24	6	11	2.9	2.5	1	$C_3A<8\%$; $C_3S+C_3A<58\%$
III	57	19	10	7	3	3.1	1.3	Higher amounts of C_3S and C_3A to promote early strength formation; $C_3A<15\%$
IV	28	49	4	12	1.8	1.9	0.8	$C_3A<7\%$; $C_3S<35\%$; $C_3S>40\%$
V	38	43	4	9	1.9	1.8	0.8	$C_3A<5\%$
Ia, IIa, and IIIa	Same as I, II, III with air entrainment agents							

Types of Portland cements

Not all cements are equal and because of differences in composition the ASTM defines eight types of Portland cements shown in Table 2, suitable for different applications. Type I Portland cement is a normal, general-purpose cement suitable for all uses. It is used in general construction projects such as buildings, bridges, floors, pavements, and other precast concrete products. Type IA Portland cement is similar to

Type I with the addition of air-entraining properties. Type II Portland cement generates less heat at a slower rate and has a moderate resistance to sulfate attack. Type IIA Portland cement is identical to Type II and produces air-entrained concrete. Type III Portland cement is a high-early-strength cement and causes concrete to set and gain strength rapidly. Type III is chemically and physically similar to Type I, except that its particles have been ground finer. Type IIIA is an air-entraining, high-early-strength cement. Type IV Portland cement has a low heat of hydration and develops strength at a slower rate than other cement types, making it ideal for use in dams and other massive concrete structures where there is little chance for heat to escape. Type V Portland cement is used only in concrete structures that will be exposed to severe sulfate action, principally where concrete is exposed to soil and groundwater with a high sulfate content1.

Portland cement and Portland cement slurries properties

Relevant properties of Portland cements are specified by the ASTM for each type of cement. Some of the properties include fineness, consistency, setting time, compressive and tensile strength, yield point and plastic viscosity.

(1) Fineness pertains to the particle size distribution. It is closely related to the surface area of the particles (i.e., the finer the cement the higher the surface area of its particles.) Fineness affects the hydration rate (setting) and the requirements for the amounts of water, retarder and dispersant in cementing because of the surface available for hydration, causing greater early strength and more rapid generation of heat (for example, fineness of type III is higher than that of type I cement.)

(2) Consistency is a rheological property related to the cohesion of the individual particles of a given material, its ability to deform, its resistance to flow, and the ability of hardened cement paste to retain its volume after setting. Consistency of cement slurries is determined by thickening-time tests in accordance with API Recommended Practice 10B and is expressed in Bearden units of consistency (Bc).

(3) Setting time: When cement is mixed with water , the cement starts stiffening until it becomes unworkable. This process is known as setting and the amount of time it takes is known as setting time.

(4) Compressive and tensile strength are the capacity of a material to withstand axially directed pushing and pulling forces respectively. When the limit of compressive or tensile strength is reached, cements are crushed. Portland cement has relatively high compressive strength, but significantly lower tensile strength (about 10% of the compressive strength). As a result, it fails from tensile stresses even when loaded nominally in compression.

(5) Portland cement slurries are Bingham plastics characterized by two parameters: yield point and plastic viscosity. Yield point (YP) is the yield stress extrapolated to a shear rate of zero on a shear rate vs. shear stress plot. Plastic viscosity (PV) is the slope of the shear stress/shear rate line above the yield point. In oil-well cementing these parameters can be modified with additives but generally they are mostly affected by the relative amount of solids in the slurry.

Cementing in oil industry

Portland cement compositions are commonly utilized in construction and subterranean applications. In particular, subterranean applications include, but are not limited to, subterranean well completion and remedial operations. For instance, cement compositions are also used in primary cementing operations whereby pipe strings such as casings and liners are cemented in well bores.

In performing primary cementing, hydraulic cement compositions are pumped into the annular space between the walls of a well bore and the exterior surface of the pipe string disposed therein. To ensure that the annular space is completely filled, a cement slurry is pumped into the annular space until it circulates to the surface. The cement composition is then permitted to set in the annular space, thereby forming an annular sheath of hardened substantially impermeable cement. The hardened cement supports and positions the pipe string in the well bore and bonds the exterior surfaces of the pipe string to the walls of the well bore[1].

Polyalkenoate Cements

Polyalkenoate cements are the result of a reaction, generally in aqueous solution, between a polyalkenoic acid (for example, poly(acrylic acid)) and a metal or mineral oxide base[2-]. Hardening can occur by reacting the base with an already-formed polymeric acid, or polymerization and neutralization can occur more or less simultaneously. Specific examples of metal oxides that have resulted in hardened polyalkenoate cements with poly(acrylic acid) include ZnO, Al_2O_3, and CuO. These cements also retain their mechanical strength when placed in contact with water as opposed to cements made from

MgO, CaO, BaO and SrO that soften upon exposure to water[5].

Polyalkenoic Acids

Polyalkenoic acids are the result of a free radical polymerization of alkenoic acids (i.e., carboxylic acids derived from alkenes) units such as maleic acid, itaconic, acrylic, etc. (see Figure 1.) Free radical polymerization is a type of polymerization in which the reactive center (i.e., the point of propagation for a growing polymer chain) is a radical (i.e., molecular or atomic species with an unpaired electron). For this process monomers containing a double or triple carbon-carbon bond, and an initiator to form the radicals, are needed. Initiators are typically organic peroxides, azo initiators, or photosensitive molecules that break up into radicals (see Figure 2.)

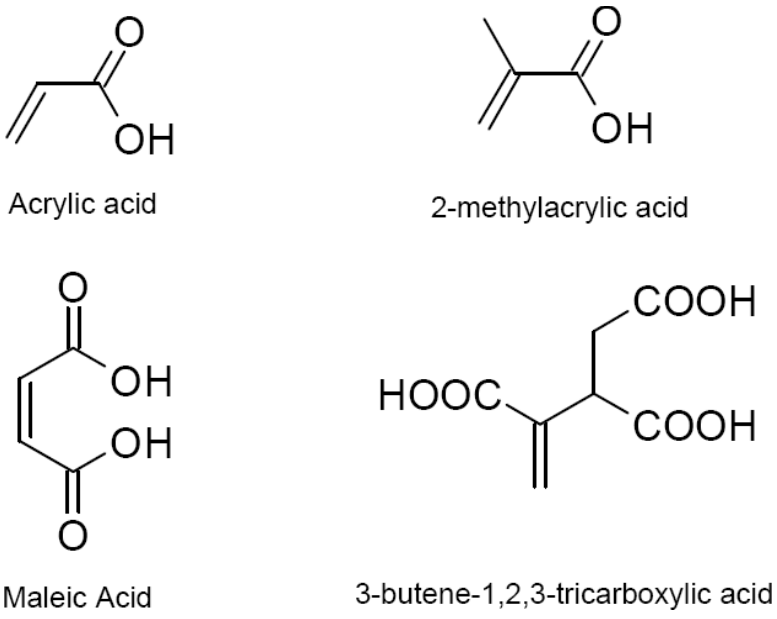

Figure 1. Suitable monomers for polyalkenoic acids manufacturing

A

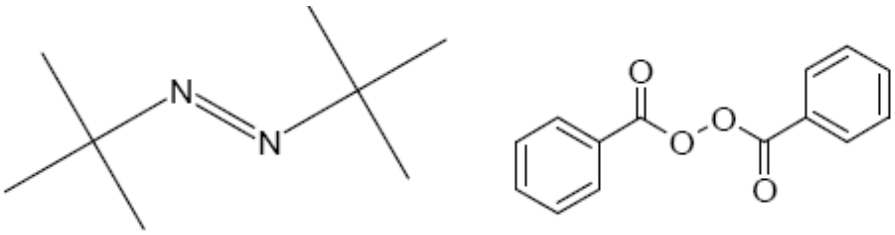

azobisisobutyronitrile (AIBN) dibenzoyl peroxide

B

Initiation	$I \rightarrow 2R\bullet$
Propagation Steps	$R\bullet + M \rightarrow RM\bullet$ $RM_n\bullet + M \rightarrow RM_{(n+1)}\bullet$
Termination	$RM_n\bullet + RM_m\bullet \rightarrow RM_{(n+m)}$

Figure 2. Examples of initiators and mechanism for free radical polymerization

Free radical polymerization mechanism consists of a series of steps which are: initiation, where two free radicals emerge from the initiator, propagation steps, where a free radical is bound to a monomer unit to form a radical-monomer,and where the radical-monomer units grow, and termination, where two radical-monomer groups collide with each other to end the reaction (see Figure 2b).

Setting of polyalkenoate cements

The cement-forming reaction of polyalkenoate cements are much more complex than that of hydraulic cements as it takes place in a number of overlapping stages. These are the acid attack on the oxide or glass, the migration of liberated ions from the oxide or glass into the aqueous phase, ionization of the polyacid with consequent unwinding of the polymer chain, interaction between the charged chains and oxide or mineral glass cations leading to ion binding and gelation, and lastly the hardening phase represented by the continuation of ion binding[2, 6].

Setting results from the gelation of the poly(alkenoic acid) by metal ions liberated from the metal oxide or silicate by acid attack. Gelation of polysalts occurs as the pH of the cement increases. Clearly, these physicochemical processes result in changes in the rheology of the cement slurry as it hardens due to conformational changes in the polymer chains and hydration. As the reaction proceeds, the polymer chain (which is in random coil form) unwinds as the charge on it grows as a result of the ionization and neutralization. This contributes to the thickening of the cement paste.

Cations released become bound to the polymer chain. Countercations can either be bound to a polyanionic chain by electrostatic forces or be site-bound to specific centers. More than one type of binding is possible. Complex formation and, if the ligand is bidentate, chelate formation enhance the effect. The extent and rate of interaction between hydrated counterion and polyanion depend on polymer structure, acid, strength, conformation, degree of dissociation, and distribution and density of the ionic charge in the polymer chain. This interaction between the cations--the counterions--and the polyanion chain disrupts the hydration regions surrounding both. Desolvation of the ion

pair, which depends on the nature of the cation and the degree of neuralization, results in gelation. Gelation itself occurs suddenly when the critical conditions for the formation of an infinite random network is met, that is when there are more than two crosslinks per polymer chain[2].

Methods to prepare polyalkenoate cements vary widely. For example, in some cases a suitable filler is mixed with a poly(alkenoic acid) aqueous solution at 30-43% and then allowed to set. Commercially, the filler is mixed with dry milled poly(alkenoic acids) and the cement is formed by mixing this powder with water. Furthermore, sometimes the filler is subjected to a deactivation process by igniting it a 900 to 1000^{o}C for 12 to 24 hours until the activity is reduced to an acceptable level. Also, an active filler might be mixed with another agent (MgO) to form a sintered mass which is ground and reheated for 8-12 hours. Sometimes sodium dihydrogen phosphate was added to the liquid to reduce the viscosity of the cement paste and to retard the setting time possibly because of the slow dissolution of the solid polyacid.

Polyalkenoate cement examples

The best known commercial example of a polyalkenoate cement is where the base is an acid-soluble glass (e.g., aluminosilicate); this material is used commonly as replacements for amalgams for dental fillings. These cements have either one or two separate hardening mechanisms. One hardening process is due to crosslinking between carboxylic acid groups by cations leached from the glass (e.g., Al^{3+})[3, 4, 7]. Some cements have additional covalent crosslinking through free-radical polymerization of pendant reactive sites extending out from the main chain. The latter types of cements are termed resin-modified glass ionomer cements.

The effect of curing time, glass powder/polymer liquid ratio, polymer molecular weight and concentration, conditions of pretreatment of the glass powder, etc., on the properties of the cement have been studied extensively[8-]. Crosslinks that form by a reaction of carbon-carbon double bonds, that are present due to the existence of a comonomer in the original synthesis of the polyalkenoic acid, can be used as well. This modification leads to significant improvements in cement toughness and flexibility[16-]. Other factors like curing time and molecular weight of the polymeric matrix in the formulation can also be very important[9, 19-]. As a point of reference to this work, dental cements can withstand compressive stresses of a magnitude 35-70 MPa[15, 22].

Theoretically many different acid-base cements could be manufactured when considering the vast amount of possible permutations of acids and metal oxides. However, the choice of a metal oxide seems to be limited by the hydrolysis constant of the cation which determines its hydrolytic stability and therefore the mechanical integrity of the resulting polyalkenoate cement. Table 3 shows some values of hydrolysis constants for cations typically encountered in polyalkenoate cements[23, 24].

To expand the applications available for polyalkenoates, research with low cost or alternative fillers has been undertaken[9, 20, 25]. Certain basic orthosilicates like willemite and gadolinite, and low iron content waste gasifier slags have been reported to produce hardened polyalkenoate cements. Compositions that contained cations with low tendency to hydrolize (e.g., Ca^{2+}, Mg^{2+}) generally lead to poorly-formed cements. In particular, Nicholson showed that the presence of iron hinders the hardening of polyalkenoate cements which was attributed to the fact that iron hydrolyzes too fast leading to the acceleration of the setting reaction and preventing optimal mixing between the filler and the polymeric matrix[26]. Additionally, iron has been seen to terminate free radical

polymerization reactions resulting in short chain polymers and compromised mechanical properties[27].

Table 3. Hydrolysis constants

Cation	**pK_h**
Na^+	14.48
Ca^{2+}	12.70
Mg^{2+}	11.42
Mn^{2+}	10.70
Zn^{2+}	9.60
Cu^{2+}	7.53
Al^{3+}	5.14
Fe^{3+}	2.19
Mn^{3+}	0.055

Despite limitations on the filler choice, previous research shows that polyalkenoate cements can be formed from non-cement forming fillers suspended in polyalkenoic acids by the addition of cation sources and other additives like tartaric acid[28]. Additionally, It has been shown that certain manganese oxides can coordinate with organic acids to produce carboxylate salts[29]. The surface of hausmannite is covered by a manganite-like

layer consistent with the fact that Mn^{3+} tends to be the favored oxidation state at the surface in manganese tetraoxide[30]. However, in a low pH environment, such as that found in solutions of aluminum chloride in water, this layer is quickly broken and Mn^{2+} becomes the prevalent species from hausmannite in solution[31, 32]. Therefore, a tentative hypothesis for the hardening of this polyalkenoate cement involves partial neutralization of the acidic solution by the basic hausmannite[33], followed by polyalkenoic acids reacting with both Al^{3+} and Mn^{2+}. This paper describes the spectroscopic characterization of these hausmannite-based polyalkenoate cements, with the aim of gaining insight to the hardening mechanism of cements where the filler is added prior to polymerization. Subsequent chapters deal with design of experiments and multivariable regression analysis to develop a hausmannite based polyalkenoate and its characterization by FTIR and XPS to verify the hypotheses outlined.

CHAPTER 2

EXPERIMENTAL

Materials

Tech grade 99.25% wt. acrylic acid (AA) containing phenothiazine as an inhibitor was purchased from Celanese (Clear Lake, TX) and was used as received, i.e. without inhibitor removal. Aluminum chloride hexahydrate 98% by weight and KBr FTIR grade were purchased from Sigma Aldrich (Saint Louis, MO). Hausmannite (Mn3O4) was obtained from Elkem (Pittsburgh, PA). 2,2'-Azobis(2-amidinopropane) dihydrochloride (V-50, WAKO Chemicals USA) was used as the initiator. Class F fly ash was supplied by ISG Resources (Tatum, TX). Tech grade 49% wt. poly(acrylic acid) (PAA) solution with 5000 g/mol molecular weight was obtained from Scientific Polymer Products (Ontario, NY.) The choice of filler materials was dictated by their cost and common usage in the oil-cementing industry.

Methods

Factorial Design of Experiments and Multivariable Regression Analysis

Due to the large number of independent variables, the most efficient approach, in our opinion, was to use a factorial design of experiments along with targeted searches to find the most useful ranges for the independent variables. In other words, a series of experiments was done according to a design of experiments methodology and the results examined. Then, a new series of experiments was performed, with the type and range of

variables studied based on the results of previous experiments. For reasons that will become clear, dependent variables were also targeted. First we studied the rheology mostclosely, then compressive properties and finally mechanical properties in tension. Of course, there was some iteration back and forth. This iterative approach allowed us to most efficiently achieve the goal of developing a replacement for Portland cement with high strength and flexibility at the most reasonable cost. Factorial design of experiments (DOE) is a powerful tool for scientific research that has been used to tackle similar problems in cement composition determination[34, 35].

DOE aims to investigate the effect of a given set of independent variables (factors) on a set of dependent variables (response variables). In a complete factorial design of experiments, all possible factor combinations are included. Thus, if p factors are investigated at q values (levels) each, q^p experimental trials are required. In this project, the designs of experiments were conducted so that no more than four factors ($p \leq 4$) and two levels ($q=2$) were studied per design of experiment. Two-level DOE use coded variables for the factors that take values of -1 and +1 for the low and high levels respectively. After data treatment the results are fitted and presented in a mathematical equation of the form:

$$y = \bar{y} + F_1 f_1 + F_2 f_2 + \cdots + F_{12} f_1 f_2 + \epsilon \qquad (1)$$

Where y is a dependent variable (e.g., plastic viscosity, yield point, maximum compressive strength etc.) ε is the error that can be estimated as having the order of three standard deviations (i.e., $\varepsilon = 3S_T$), f subscripted represents the factors (filler volume percentage, initiator ratio, cation ratio etc.) and F subscripted are numerical coefficients bearing the same units as the dependent variable. A coefficient accompanying a single independent variable is termed effect (e.g., F_1, F_2, etc.) and a coefficient accompanying a

product of two or more independent variables is called interaction (e.g., F_{12}, F_{123}, etc.) Not all coefficients are statistically significant; coefficients smaller than three standard deviations were deemed insignificant and discarded. Two methods were used to estimate the error of the statistical samples: with replicates of runs and by neglecting interactions of three or more factors[36]. For the first method, the standard deviation S_T^2 was determined by first calculating the variance s_i^2 for the set of conditions i as shown in formula (2).

$$s_i^2 = \frac{(y_{i_1} - \bar{y}_i)^2 + \cdots + (y_{i_r} - \bar{y}_i)^2}{(r_i - 1)} \qquad (2)$$

Where r_i is the number of replicates run for that particular set of conditions i and $\bar{y}_i$ is the average value calculated from:

$$\bar{y}_i = \frac{\sum_{j=1}^{r_i} y_{i_j}}{r_i} \qquad (3)$$

The variance for a design of experiments is determined by averaging the calculated standard deviations, weighted appropriately. The weighting factors are the degrees of freedom on each run given by the formula:

$$v_i = r_i - 1 \qquad (4)$$

So that the variance for the DOE is:

$$S_T^2 = \frac{\sum_{i=1}^{N} v_i s_i^2}{\sum_{i=1}^{N} v_i} \qquad (5)$$

N represents the total number of i conditions, each having r_i replicates.

When there are no replicates in a DOE, a direct measure of the variance is not possible. However, the variance can be estimated if the assumption is made that

highorder interactions are insignificant. In particular, if all three variable (F_{123}, F_{124}, F_{234}, etc.) and higher number of variable interactions are assumed to be negligible, these coefficients would quantitatively be related to the experimental error. This set of interactions could provide an appropriate reference set for the remaining effects as shown by Box[36], although this procedure has a tendency to overestimate the actual standard deviation because it uses the predicted value by the model of the dependent variable to calculate the standard deviation instead of the average value of a run (i.e., the estimate depends largely on how good is the fit provided by the model.) Formula (6) shows the calculation of the variance with no replicates:

$$S_T^2 = \frac{\sum [COEFFICIENTS]_i^2}{N_{COEFFICIENTS}} \qquad (6)$$

One limitation of factorial DOE is that the conclusions are applicable only to conditions set for the experiment and no extrapolations nor interpolations are acceptable from the statistical point of view. Looking at this issue from another direction, the model will be accurate only if the dependent variables are linearly dependent on factors and two-variable interactions. As stated earlier, our approach to this problem was to use a DOE to identify useful areas for experimentation and then conduct new DOEs to either fill in regions that were within the range of the previous experiment(s) or go outside the range to investigate promising areas of variable space. Economic considerations were extremely important when deciding which areas to study. With this approach, each DOE has its own model equations. In order to draw more universal conclusions, all data was combined into one data set, the independent variables recoded and the set was then subjected to a multivariable regression analysis for each dependent variable. Each ingredient amount (i.e., filler, initiator, cation source, water etc.) can be considered an

independent variable. However, working with relative amounts means that the results do not depend on the overall amount of the formulation. The key issue is defining a normalizing factor; we chose the monomer amount because the polymerized product from this component binds the composite matrix. Time was also included among the factors to be studied. All factors and dependent variables are found in Table 4.

Table 4. Factors and dependent variables for design of experiments (DOE) and multivariable regressions

FACTORS	***SYMBOL***
Cation ratio (mol Acrylic acid / mol Cation)	***C***
Monomers ratio (g Acrylic acid / g MBA)	***M***
Fiber ratio (vol. Fibers / (vol. Hausmannite + vol. Fly ash)	***F***
Filler type ratio (vol. Hausmannite / vol. Fly ash)	***FR***
Filler ratio (vol. Acrylic acid / vol. Filler)	***G***
Filler volume percentage (vol. Filler(s) / vol. Slurry)	***FVP***
Initiator ratio (mol Monomer (total) / mol Initiator)	***I***
Water ratio (vol. Acrylic acid / vol. water)	***W***
Time (hours)	***T***
DEPENDENT VARIABLES	***SYMBOL***
Plastic viscosity (mPa s)	***PV***
Yield point (Pa)	***YP***
Maximum compressive stress (MPa)	y_1
Compressive modulus (MPa)	y_2
Compressive failure strain (%)	y_3
Maximum tensile stress (MPa)	y_4

Plastic viscosity and yield point were used assuming that the rheological response is well described by the Bingham model. Aluminum chloride was selected because aluminum is multivalent and $AlCl_3$ is relatively inexpensive and soluble in water. It was

initially thought that the type of filler would not be crucial to the hardening of the cement. Iron (III) oxide, hausmannite, quartz, fly ash and acid-degradable glass were tested. Of these fillers, only hausmannite (Mn_3O_4) and acid-degradable glass produced hardened materials. In order to help reduce the cost of the final formulation, the low-cost filler fly ash was mixed with hausmannite and its properties investigated as well.

Mixing

For the mechanical properties and rheology tests using design of experiments, solid materials were placed in a variable speed laboratory blender from Waring Laboratory Equipment (Torrington, CT) and mixed together dry at 1000 RPM. The stabilizer dose was adjusted to 0.01 g Xanthan gum/g fillers to keep all solids suspended. The azo initiator was dissolved with tap water at room temperature. After dissolution, the initiator was added with the aluminum chloride solution, water and acrylic acid to the premixed dry ingredients and mixed for 5 minutes, or until no lumps of solid material were detected in the slurry, at 3000 RPM. 100 ml of monomer was used for most formulations, resulting in a wet basis formulation size of approximately 300 ml, depending on the exact amount of ingredients used as determine by the DOE model being tested.

Rheology

The yield point and plastic viscosity were measured per API recommended practice 10B using a Fann 35A rotational viscometer (Houston, TX) immediately after mixing.

Mechanical Properties

Cement substitute slurries were poured in plastic cylindrical molds with 2.54 cm diameter or into dog-bone shaped molds, depending on the test to be run. These samples

were placed in an autoclave pressure regulated with nitrogen and allowed to harden at 60°C and 7 MPa. Compressive and tensile strength were measured in the hardened cylindrical and dog-bone shaped samples per ASTM standards C109 and C190-85 respectively using a Tinius Olsen CMH 496 press (Horsham, PA).

Polyalkenoate Samples Preparation for Characterization by XPS and FTIR

Samples of 10 mL consisting of 2 g of Mn_3O_4 and $AlCl_3$ at concentrations of 0, 0.25, 0.5, 0.75 M were prepared to evaluate surface coverage of aluminum on hausmannite. Samples of 10 mL with 1 g of hausmannite in acrylic acid at 4.4 eq/L and $AlCl_3$ at concentrations of 0 and 0.5 M were prepared to evaluate coordination of acrylic acid with hausmannite, surface coverage of aluminum on hausmannite, and ionic crosslinking with Al^{3+} or Mn^{2+}. A similar set of 10 mL samples with 1 g of hausmannite was prepared with poly(acrylic acid) at 5.6 eq/L, and $AlCl_3$ at concentrations of 0 and 0.5 M. All samples were mixed and allowed to equilibrate for three days in capped centrifuge tubes at ambient temperature. The slurries were then centrifuged to separate solids from the liquid. The solids were dried at 80°C and atmospheric pressure for two days. These samples turned out to be hardened solid masses that had to be pulverized for FTIR and XPS analysis. Samples of 100 mL in size with the compositions shown on Table 5 were also prepared and cured as described previously under nitrogen blanketing at 1000 PSI and 60ºC to ensure hardening. Compressive strength was measured in the hardened samples using a Tinius Olsen CMH 496 press (Horsham, PA). These samples were also pulverized for XPS and FTIR analysis.

Table 5. Hausmannite-based polyalkenoate cements formulations

Formula	Hausmannite (g/100 mL)	Microflyash (g/100 mL)	[AA] (M)	[$AlCl_3$] (M)	[Initiator] (mM)
1	80	-	4.8	0.5	3.7
2	80	-	4.8	0.12	3.7
3	40	35	4.8	0.5	3.7
4	40	35	4.8	0.12	3.7

Characterization by XPS and FTIR

Samples for FTIR were prepared by mixing 0.4 g of FTIR grade KBr and 0.001 g sample and then pressed into pellets at ambient temperature and 9000 PSI using a pneumatic press. FTIR spectra were collected using a Genesis FTIR. XPS data were recorded on a Physical Electronics PHI 5800 ESCA System with a background pressure of approximately 3.0×10^{-9} Torr. The electron takeoff angle was 45^{o} with respect to the sample surface. A spot size of 0.8 mm and 23 eV pass energy were used for the analysis. The binding energies were corrected by reference to the C1s line at 284.8 eV for hydrocarbon. Quantification of the surface composition was carried out by integrating the peaks corresponding to each element with aid of the Shirley background subtraction algorithm, and then converting these peak areas to atomic composition by using the sensitivity factors provided for the each element by the PHI 5800 system software.

CHAPTER 3

MECHANICAL PROPERTIES AND RHEOLOGY MODELING

Rheology

To successfully place the cement in a desired location often requires control of the cement slurry viscosity. One of the first experiments was a DOE, shown in Table 6, geared at determining the effect of the filler, cation and initiator on the yield point and the plastic viscosity for those conditions that yielded hardened samples. Formulas (7) and (8) show how to calculate the plastic viscosity (*PV*) and yield point (*YP*):

$$PV(mPa\,s) = 1.5(READING_{300\,RPM} - READING_{100\,RPM}) \qquad (7)$$

$$YP(Pa) = 4.788(READING_{300\,RPM} - PV(mPa\,s)) \qquad (8)$$

Simple inspection by comparing gray rows with clear rows on Table 6 shows that the rheology of the cement slurries depends primarily on the filler volume percentage; a similar result has been reported for Portland cement slurries[37]. Experiments were performed to better bracket this dependence for hausmannite. The result of this study was the observation that a filler volume percentage of 22% yields values for *PV* and *YP* required for oil-well cementing at the average values of the parameters listed in Table 6.

The values of the parameters used in Table 6 were not those that yielded the best product. To better test the premise that only filler volume percentage affects the rheological properties of the cement slurry in the operating range of interest, the filler volume percentage was fixed at 22% and the initiator and cation ratios were changed as shown in Table 7.

Table 6. 2^3 DOE for rheology dependence on filler, cation, and initiator ratios and on the filler volume percentage

EXPERIMENTAL CONDITIONS			
VARIABLES	**-1**	**+1**	
Filler ratio (G)	2	4	vol. Monomer / vol. Filler
Cation ratio (C)	10	100	mol Monomer / mol Cation
Initiator ratio (I)	1000	1500	mol Monomer / mol Initiator
FIXED PARAMETERS			
Water ratio (W)	1	vol. Monomer / vol. Water	

RUN	**G**	**C**	**I**	**Filler Volume Percentage (%)**	**PV (mPa s)**	**YP (Pa)**
1	-1	-1	-1	19.76	11.42	79.15
2	+1	-1	-1	10.96	10.73	18.53
3	-1	+1	-1	19.98	11.25	80.53
4	+1	+1	-1	11.1	10.72	19.25
5	-1	-1	+1	19.76	11.51	82.40
6	+1	-1	+1	10.96	10.80	17.57
7	-1	+1	+1	19.98	11.55	80.20
8	+1	+1	+1	11.1	10.51	20.11

AVERAGES	$\bar{FVP}$ **(%)**	$\bar{PV}$ **(mPa s)**	$\bar{YP}$ **(Pa)**
GRAY ROWS	19.87 ± 0.13	11.43 ± 0.13	80.57 ± 1.36
CLEAR ROWS	11.03 ± 0.08	10.69 ± 0.13	18.86 ± 1.08

Although the other variables do affect the rheology, the filler volume percentage has a much stronger effect on the rheology than either the initiator or cation ratio. As will be shown, none of the other dependent variables, i.e. the mechanical properties, have such a strong dependence on filler volume percentage. Hence, a design strategy is to formulate for rheology by adjusting the filler volume percentage and manipulate the remaining

variables to obtain cements with desired mechanical properties.

Table 7. 2^2 DOE to test rheology dependence on cation and initiator ratios

EXPERIMENTAL CONDITIONS						
VARIABLES				**-1**	**+1**	
Cation ratio (C)				10	20	mol Monomer / mol Cation
Initiator ratio (I)				2000	5000	mol Monomer / mol Initiator
FIXED PARAMETERS						
Water ratio (W)					0.8	vol. Monomer / vol. Water
Filler Volume Percentage (%)					22	vol. Filler / vol. Slurry
RUN	***G***	***C***	***I***	***YIELD POINT (Pa)***		***PLASTIC VISCOSITY (mPa s)***
1	-1	-1	-1	76.61		22.50
2	+1	-1	-1	142.44		26.25
3	-1	+1	-1	146.03		36.00
4	+1	+1	-1	260.95		54.00
RHEOLOGY				***DOE MODEL EQUATION***		
Plastic Viscosity (mPa s)				$PV = 34.69 + 5.44C + 10.31I + 3.56CI$		6-1
Yield Point (Pa)				$YP = 156.51 + 45.19C + 46.98I + 12.27CI$		6-2

What effect does the identity of the filler have on the rheological properties? Table 8 shows that *PV* and *YP* depend heavily on the hausmannite/fly ash volume ratio. The dependence is probably due to the different particle size distribution of the fly ash and the manganese tetraoxide[38, 39]. This DOE also showed that the filler volume percentage to attain *PV* and *YP* required for oil-well cementing is 26% at a 50/50 hausmannite/fly ash volume ratio.

Table 8. 2^2 DOE using flyash to verify rheology dependence on filler volume percentage, filler ratio and water ratio

EXPERIMENTAL CONDITIONS					
VARIABLES			**-1**	**+1**	
Water ratio (W)			0.6	0.8	vol Monomer / vol. Water
Filler Volume Percentage (FVP)			0.2	0.3	vol Filler(s) / vol Slurry
MM/MFA vol. Ratio (FR)			0.3	0.5	vol. Hausmannite / vol. Flyash
FIXED PARAMETERS					
Cation ratio (C)				50	mol Monomer / mol. Cation
Initiator ratio (I)				5000	mol Monomer / mol Initiator
Time (T)				22	hours
RUN	***G***	***C***	***I***	***PLASTIC VISCOSITY (mPa s)***	***YIELD POINT (Pa)***
1	-1	-1	-1	11.25	10.77
2	+1	-1	-1	10.5	19.15
3	-1	+1	-1	13.5	11.97
4	+1	+1	-1	12	19.15
5	-1	-1	+1	30	50.27
6	+1	-1	+1	50.25	89.78
7	-1	+1	+1	33	81.4
8	+1	+1	+1	29.25	73.02
RHEOLOGY				***DOE MODEL EQUATION***	
Plastic Viscosity (mPa s)				$PV = 23.72 + 11.91\text{FR} \pm 6$	7-1
Yield Point (Pa)				$YP = 44.44 + 29.16\text{FR} \pm 37.3$	7-2
Note: standard deviations were estimated by duplicates					

Mechanical Properties Modeling

Factorial Design of Experiments

Materials made according to the DOE shown in Table 8 were also used to gather mechanical properties data in compression. Some samples with a water ratio of 0.6 vol. monomer/vol. water didn't harden, indicating the lower bound of the water ratio. Mechanical properties results from hardened samples are shown in Table 9 along with a complete description of the experimental conditions. The water ratio was fixed at the minimum level required for consistent hardening, i.e. 0.8 vol. monomer/vol. water. As shown in Equations 8-1, 8-2 and 8-3, all effects have the same order of magnitude for the maximum compressive strength and compressive modulus.

For the next set of experiments shown in Table 10, the filler volume percentage was set at 26% to be within rheological constraints and the water ratio set at 0.8 vol. acrylic acid/vol. water. For the maximum compressive stress, monomer/cation ratio is the most relevant factor. Increasing the monomer/cation ratio (i.e., diminishing the amount of cation) results in samples with lower compressive strength, but higher flexibilities, consistent with observations made previously[7]. Interpreting compressive moduli results was not straightforward because of the wide range of values.

The DOE procedure inherently assumes the same same orders of magnitude for standard deviation for all runs; a large variation in the order of magnitude of the standard deviation around averaged values, means that the standard deviations for the runs are almost certainly not distributed normally. A simple expedient is to use the logarithm of the compressive modulus, i.e. calculate the logarithm of each individual value, then

average the logarithmic values. Since the standard deviation of this variable is $S_T = 0.084$ and all of the effects and interactions are larger than three standard deviations, none of them can be discarded and no firm conclusion can be established about compressive modulus.

Table 9. 2^3 DOE using flyash to study mechanical properties under compression dependence on the filler volume percentage and filler ratio

EXPERIMENTAL CONDITIONS					
VARIABLES			**-1**	**+1**	
Filler Volume Percentage (FVP)			0.2	0.3	vol Filler(s) / vol Slurry
MM/MFA vol. Ratio (FR)			0.3	0.5	vol. Hausmannite / vol. Flyash
FIXED PARAMETERS					
Water ratio (W)				0.8	vol Monomer / vol. Water
Cation ratio (C)				50	mol Monomer / mol. Cation
Initiator ratio (I)				5000	mol Monomer / mol Initiator
Time (T)				22	hours
RUN	***FVP***	***FR***	***MAX. COMP. STRESS (MPa)***	***COMP. MOD. (MPa)***	***FAIL STRAIN (%)***
2	+1	-1	0.78	1.48	52.68
4	+1	+1	1.06	11.16	17.07
6	+1	-1	5.38	9.62	51.22
8	+1	+1	0.93	17.67	8.05
PROPERTIES MODELING			***DOE MODEL EQUATION***		
Max. compressive stress (MPa)			$y_1 = 2.04 - 1.04\,FVP + 1.12\,FR - 1.18\,FR \cdot FVP$		8-1
Compressive modulus (MPa)			$y_2 = 9.98 + 4.43\,FVP + 3.66\,FR - 0.41\,FR \cdot FVP$		8-2
Failure Strain (%)			$y_3 = 32.26 - 19.7\,FVP - 2.62\,FR - 1.89\,FR \cdot FVP$		8-3

Table 10. 2^2 DOE for mechanical properties models under compression dependence on the cation and initiator ratios

EXPERIMENTAL CONDITIONS								
VARIABLES			**-1**			**+1**		
Initiator Ratio (I)			2000			5000		mole Monomer / mole Initiator
Cation Ratio (C)			10			20		mole Monomer / mole Cation
FIXED PARAMETERS								
Water Ratio (W)						0.8		vol. Monomer / vol. Water
MM/MFA vol. Ratio (FR)						0.5		vol. Hausmannite / vol. Fly ash
Filler Volume Percentage (FVP)						26%		vol. Filler(s) / vol. Total
Time (T)						17		hours
RUN	***C***	***I***	***MAXIMUM COMP. STRESS (MPa)***				$\bar{y}_i$ **(MPa)**	s_i^2
1	-1	-1	3.92	3.87	4.50	4.32	4.15	0.09
2	+1	-1	8.64	12.13			10.39	6.11
3	-1	+1	9.54	9.92	9.09		9.52	0.17
4	+1	+1	13.75	13.52			13.63	0.03
							S_T^2 =	0.91
RUN	***C***	***I***	***COMPRESSIVE MODULUS (MPa)***				$\bar{y}_i$ **(MPa)**	s_i^2
1	-1	-1	193.68	182.61	236.72	206.17	204.80	545.49
2	+1	-1	243.48	241.45			242.47	2.05
3	-1	+1	639.14	568.13	613.63		606.97	1294.13
4	+1	+1	338.17	306.34			322.26	506.67
							S_T^2 =	676.18
RUN	***C***	***I***	***COMPRESSIVE FAILURE STRAIN (%)***				$\bar{y}_i$ **(%)**	s_i^2
1	-1	-1	3.00	3.25	3.00	3.25	3.13	0.0209
2	+1	-1	7.00	8.00			7.50	0.5
3	-1	+1	2.50	3.38	8.50		4.79	10.50
4	+1	+1	9.50	10.00			9.75	0.125
							S_T^2 =	3.08

PROPERTIES MODELING	***DOE MODEL EQUATION***	
Maximum compressive stress (MPa)	$y_1 = 9.42 - 2.59C + 2.15I \pm 2.86$	9-1
Compressive modulus (MPa)	$y_2 = 344.12 - 61.76C + 120.49I - 80.6CI \pm 78.01$	9-2
	$\ln y_2 = 5.75 - 0.11C + 0.34I - 0.2CI \pm 0.24$	9-3
Failure Strain (%)	$y_3 = 6.29 - 2.33C \pm 1.76$	9-4

A more elaborate design of experiments than the previous ones is shown in Table 11. Since the monomer/cation ratio effect on some of the mechanical properties can be explained by crosslinking of the polymeric matrix, the ratios were increased (i.e. the amount of cation reduced) to increase the flexibility of the cement matrix. The levels of the initiator remained unchanged because the relative effect of this variable is negligible compared to the remaining variables. Hardening times were arbitrarily chosen to be 20 hours and 44 hours under pressure for the low and high levels of the DOE respectively. The variance was determined using the values of the coefficients of the three and four-variable interactions.

Consistent with the previous DOE, a linear model for the compressive modulus does not fit the data very well, while the other dependent variables are well fit by linear models. Time is clearly the most important variable in describing the compressive strength, i.e. the compressive strength builds slowly over time. Figure 3a shows that despite having a single factor (i.e., time) the data for the maximum compressive strength is modeled adequately by equation 10-1. The increase in maximum compressive strength with time is accompanied by a decrease in failure strain, also well described by the model as shown in Figure 3b. As before, increasing the monomer/cation ratio increases the failure strain of the samples while the initiator has no impact on the failure strain of the samples. Finally, increasing the amount of monomer by increasing the water ratio does not yield significant improvements in mechanical properties, which is encouraging since increasing monomer increases the cost of the cement. Figure 3, parts C and D show the modeling for the compressive modulus using linear and logarithmic models. Not only does the logarithmic model better predict the compressive modulus, but only positive values result. However, the logarithmic model for compressive modulus cannot be

established with 16 runs and no replicates.

Table 11. 2^4 DOE for mechanical properties under compression

EXPERIMENTAL CONDITIONS							
VARIABLES					**-1**	**+1**	
Cation Ratio (C)					20	50	mole Monomer / mole Cation
Initiator Ratio (I)					2000	5000	mole Monomer / mole Initiator
Water Ratio (W)					0.8	1.0	vol. Monomer / vol. Water
Time (T)					20	44	hours
FIXED PARAMETERS							
Hausmannite/Fly ash Ratio (FR)						0.5	vol. Hausmannite / vol. Fly ash
Filler Volume Percentage (FVP)						26	vol. Filler(s) / vol. Total
RUN	***C***	***I***	***W***	***T***	***MAX. COMP. STRESS (MPa)***	***COMP. FAIL. STRAIN (%)***	***COMPRESSIVE MODULUS (MPa)***
1	-1	-1	-1	-1	9.54	8.25	139.19
2	+1	-1	-1	-1	6.43	30.58	21.98
3	-1	+1	-1	-1	8.63	8.25	152.17
4	+1	+1	-1	-1	4.89	12.74	16.49
5	-1	-1	+1	-1	18.48	14.20	347.19
6	+1	-1	+1	-1	8.67	28.16	29.39
7	-1	+1	+1	-1	1.60	17.96	40.58
8	+1	+1	+1	-1	8.88	29.13	28.41
9	-1	-1	-1	+1	16.20	3.88	671.10
10	+1	-1	-1	+1	16.00	12.74	227.25
11	-1	+1	-1	+1	15.51	3.40	869.95
12	+1	+1	-1	+1	14.69	17.48	150.39
13	-1	-1	+1	+1	25.65	4.85	958.72
14	+1	-1	+1	+1	16.89	15.05	147.95
15	-1	+1	+1	+1	3.71	2.18	142.03
16	+1	+1	+1	+1	17.10	19.42	112.13

PROPERTIES MODELING	***DOE MODEL EQUATION***	
Maximum compressive stress (MPa)	$y_1 = 12.05 + 3.66\,T \pm 3.48$	10-1
Compressive modulus (MPa)	$y_2 = 253.43 - 161.68\,C + 156.51\,T \pm 147.28$	10-2
	$\ln y_2 = 4.84 - 0.74\,C + 0.82\,T \pm 0.41$	10-3
Failure Strain (%)	$y_3 = 14.27 + 6.4\,C - 4.39\,I \pm 3.94$	10-4

The maximum tensile stress of the samples was still not acceptable (i.e., a sample prepared with Portland Cement class III yielded a tensile strength of 500 PSI) and for this reason a nonionic, organic crosslinking comonomer, N,N'-methylenebisacrylamide (MBA) and glass fibers were added to the formulations and the results of tests involving those variables are shown in Tables 12 and 13. Glass fibers reduced the maximum compressive stress and the compressive failure strain and since glass fibers are more expensive than manganese tetraoxide, glass fibers were not added to the formulations hereafter. On the other hand, MBA comonomer increased significantly the maximum compressive stress and the compressive modulus without a significant change in failure strain.

The reason for studying tensile mechanical properties only after determining the best properties from compression is that we were sample limited in the former case; only two dog-bone samples could be fit in the autoclave, while eight cylindrical compression samples would fit. For the same reason, the standard deviation of tensile strength was not estimated as with other properties due to lack of replicates. Cation amount was also added as a variable. Cation amount was added as a test variable because both cation and comonomer cause crosslinking. The fact that the interaction *CM* is of the same order of magnitude of the effect M in equation 12-1 indicates that *CM* can't be discarded and is evidence of competition with respect to crosslink sites between MBA and the cation source.

The most interesting result of this set of experiments was that the addition of MBA comonomer significantly increased the tensile strength as it did the compressive strength, without any noticeable change in failure strain. At higher amounts of cation (runs 1 and 3), the addition of MBA changes the tensile strength very little, while at lower amount of

cation source (runs 2 and 4) MBA has a large effect on the measured tensile strength. An increase in fracture toughness with the addition of moieties containing pendant double bonds, as found here, is typical for resin-modified glass ionomer dental cements vs. conventional glass ionomer cements[40-]. The reason for this improvement in toughness is not clear. Since both poly(acrylic acid) and poly(N,N'-dimethylacrylamide) are glasses at room temperature, the behavior is not expected to be the result of increased main-chain flexibility. One complicating factor is that aluminum leads to a minimum of a three-functional crosslink, while the MBA crosslink is two functional. Further, the location of the crosslink relative to the main chain is different as well for the two types of crosslinks.

Multivariable Linear Regression

All runs were gathered together and one mathematical model was fit to all the data for each dependent variable using SAS graph (v. 5.0). A total of 59 data points exist for the mechanical properties under compression with the factors defined in Table 14. The linear model in Equation (15) was used:

$$y=\beta_0+\beta_1 C+\beta_2 M+\beta_3 FR+\beta_4 F+\beta_5 FVP+\beta_6 I+\beta_7 W+\beta_8 T+\epsilon \quad (9)$$

Prior to the multivariable regression analysis colinearity was tested and not detected. The adequacy and fitting of the data with the model were tested subsequently. This is important because this reflects how independent variables affect a dependent variable and how well a regression equation fits the data. In order to assess how well the data is fit by the model the coefficient of determination ($0<R^2<1$) is used. Values of R^2 approaching 1 are desirable as this indicates a good fit of the data. However, it is not enough to have a good fit for the data, because by increasing the number of parameters (by, for example, adding interactions) R^2 can be improved.

Table 12. 2^3 DOE for mechanical properties under compression using glass fibers and methylenebisacrylamide (MBA)

EXPERIMENTAL CONDITIONS			
VARIABLES	**-1**	**+1**	
CURING TIME (T)	24	48	Hours
FIBERS RATIO (F)	0.05	0.30	Vol. FIBERS / Vol. FILLER(S)
MONOMERS RATIO (M)	3.33	20	mol Acrylic Acid / mol MBA
FIXED PARAMETERS			
FILLER+FIBERS VOL. PERCENTAGE (FVP)	26	vol. filler(s) / vol. slurry	
CATION RATIO (C)	50	mol acrylic acid / mol cation	
INITIATOR RATIO (I)	2000	mol monomers (total) / mol initiator	
WATER RATIO (W)	0.8	vol. Acrylic Acid / vol. water	
HAUSMANNITE/FLY ASH RATIO (FR)	0.5	vol. hausmannite / vol. flyash	

RUN	***C***	***I***	***T***	***COMP. FAIL STRAIN (%)***		***MAX. COMP. STRESS (MPa)***		***COMPRESSIVE MODULUS (MPa)***	
				REP 1	***REP 2***	***REP 1***	***REP 2***	***REP 1***	***REP 2***
1	-1	-1	-1	23.06	27.43	17.79	14.96	58.21	67.34
2	+1	-1	-1	18.93	19.42	13.04	14.62	64.72	71.02
3	-1	+1	-1	21.84	19.42	40.54	39.44	196.66	189.38
4	+1	+1	-1	13.59	14.08	28.68	27.99	172.47	172.47
5	-1	-1	+1	10.68	11.17	17.79	18.06	142.03	183.81
6	+1	-1	+1	11.89	12.14	17.58	18.06	97.65	97.65
7	-1	+1	+1	15.53	15.05	42.33	39.64	236.72	236.72
8	+1	+1	+1	9.71	11.65	32.27	32.34	224.89	224.89

PROPERTIES MODELING	***DOE MODEL EQUATION***	
Maximum compressive stress (MPa)	$y_1 = 25.95 - 2.87F + 9.46M \pm 2.57$	11-1
Compressive modulus (MPa)	$y_2 = 152.29 - 54.49M + 28.26T \pm 17.1$	11-2
	$\ln y_2 = 4.91 - 0.41M + 0.22T \pm 0.14$	11-3
Failure Strain (%)	$y_3 = 15.97 - 3.75T \pm 2.9$	11-4

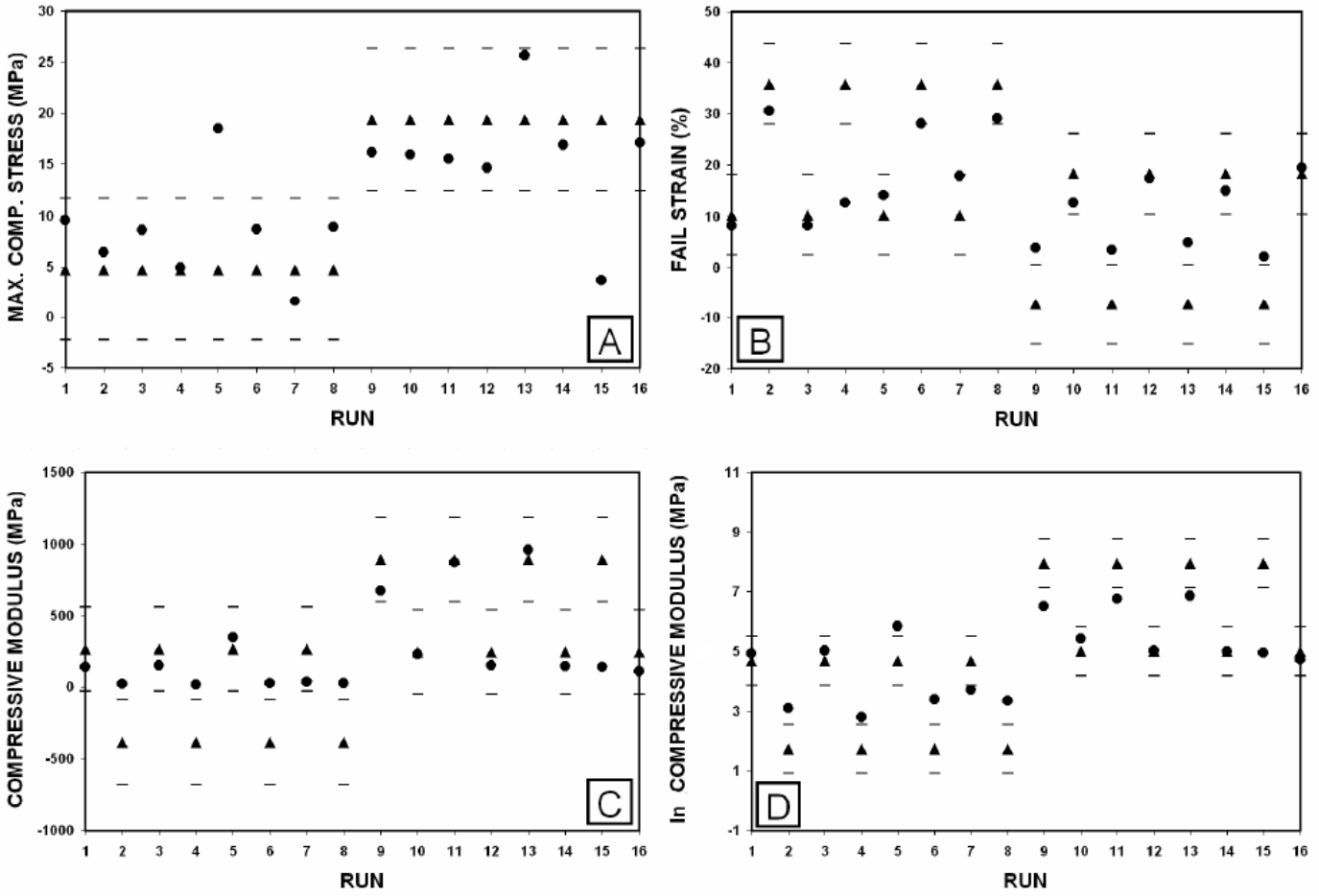

Figure 3. Graphical Representation of experiments shown in Table 10: A) Maximum Compressive Stress, B) Failure Strain, C) Compressive Modulus logarithmic model, D) Compressive Modulus linear model. Circles represent data points, triangles are predicted values and the lines are predicted values +/- three standard deviations

Table 13. 2^2 DOE for maximum tensile stress testing

EXPERIMENTAL CONDITIONS				
VARIABLES			**-1**	**+1**
Cation Ratio (C)			20	50
Monomer Ratio (M)			1.67	3.33
FIXED PARAMETERS				
Initiator Ratio (I)			2000	
Water Ratio (W)			0.8	
MM/MFA vol. Ratio (FR)			50/50	
Filler Volume Percentage (FVP)			26%	
Time (T)			72	
RUNS	***C***	***M***	***MAXIMUM TENSILE STRESS (MPa)***	
1	-1	+1	1.59	
2	+1	+1	1.36	
3	-1	-1	1.65	
4	+1	-1	2.38	
MECHANICAL PROPERTY			***DOE MODEL EQUATION***	
Maximum tensile stress (MPa)			$y_4 = 1.75 + 0.13C - 0.27M - 0.24CM$	12-1

In order to verify whether an excessive number of independent variables have been used the F statistic given by the formula shown below is used.

$$F = \frac{R^2 / v_1}{(1 - R^2)/v_2} \qquad (10)$$

υ_1 and υ_2 are the degrees of freedom given by formulas (11) and (12) below:

$$v_1 = k \qquad (11)$$

$$v_2 = N - 1 - k \qquad (12)$$

k is the number of predictors (i.e., β coefficients) except for the intercept and N is the number of observations. For the statistical analysis, the calculated value of F has to be compared with the F_α value obtained from the F-distribution tables to assess overall adequacy of the model. For this test we used a confidence coefficient α of 5% and the same degrees of freedom as above.

For example, for the first four equations of Table 14, there are 59 observations (N=59) and 8 coefficients (k=8). With α=5% and the specified degrees of freedom we find that $F_\alpha = 2.13$. To address the overall adequacy of the model the condition on formula (13) should be true:

$$|F| > F_\alpha \qquad (13)$$

Comparing this value with F for the first four equations in Table 14, it is evident that the predictor variables model well the compressive properties of the cement substitute and that the models are statistically adequate. However, the R^2 value for the compressive modulus are too low and this leads us to conclude that this dependent variable can not be fit using a linear model.

The residuals analysis (i.e., $y_i - y_i^P$ vs. y_i^P where y_i^P is the predicted value by the model and y_i a data point) of the compressive modulus on Figure 4 shows that these values are not distributed randomly. This particular funneled pattern for the residuals suggests a transformation of the dependent variable into its logarithm to fit the data. The logarithmic model and its improved statistics and R^2 (0.806 vs. 0.485) are also shown.

The next step consists of testing the null hypothesis for each coefficient in the regressions and to determine if there are grounds for considering any of the coefficients to be zero using the t-student distribution. The coefficients fulfilling the condition on formula (14) can not be neglected.

$$|t| > t_\alpha \qquad (14)$$

The value of $t_\alpha = 1.676$ is calculated using $\nu = N\text{-}1\text{-}k$ degrees of freedom (ν = 50) and α = 5%. Examining the t-values for each one of the coefficients leads us to propose models with less parameters. As can be seen the F value for the models increases dramatically, while the remaining statistics (i.e., s and R^2) are marginally affected, i.e.

the overall adequacy of the models improved.

The final step involves eliminating outliers in the data in order to improve the correlation coefficient. In this analysis, those points that fell outside of two standard deviations for the predicted value of any dependent variable were eliminated. If a sample exceeded 2 standard deviations for any dependent variable, it was eliminated for consideration from all dependent variables. The resulting sample still contains 52 data points. Table 14 also shows the resulting models after the elimination of all outliers outside two standard deviations from the predicted values. In general, the models changed minimally in their coefficients but the statistics improved. The predicted values for the failure strain after the elimination of outliers fit accurately within $y_i^P \pm 2.6s$, with five data points that do not fall within two standard deviations from the predicted value. This represents 10% of the data and is very good statistically. However, the resultant formula can give negative failure strain, which does not make physical sense. The predicted values for the maximum compressive stress are very well predicted: Only 11 data points are outside of the $y_i^P \pm s$ interval and all data can be enclosed in an $y_i^P \pm 1.7s$ interval. Remarkably, two of the points that fall outside of the one standard deviation interval have excellent mechanical properties due to the high comonomer/monomer ratio (maximum compressive stress of approximately 40 MPa and a failure strain of 14%.)

Table 14. Multivariable linear regression with statistical hypotheses analysis

EXPERIMENTAL CONDITIONS								
	-1	**+1**	***DEFINITION***					
Cation Ratio (C)	20	50	mole Acrylic Acid / mole Cation					
CoMonomer Ratio (M)	3.33	20	mole Acrylic Acid / mole MBA					
Fiber Ratio (F)	0.05	0.3	vol. Fibers / vol. Filler(S)					
Filler 1 / Filler 2 (FR)	0.78	1	vol. Hausmannite / vol. Microflyash					
Filler + fibers volume percentage (FVP)	0.26	0.3	Filler(s) + Fibers Vol./Total Vol.					
Initiator Ratio (I)	2000	5000	mole Monomers (total) / mole Initiator					
Water Ratio (W)	0.5	1	vol. Acrylic Acid / vol. Water					
Time (T)	24	48	hours					
MODEL EQUATIONS AND STATISTICS FROM SAS PROGRAMS							***F***	***s***	***R²***
MAX. COMP. STRESS (MPa)	$y_1 = 940.43 - 0.205C + 667.2M - 2.41F + 0.997FR - 0.42FVP + 0.92I + 2.42W + 2.76T$						45.38	3.984	0.879
COMP. MODULUS (MPa)	$y_2 = 3521.07 - 118.48C + 2349.5M - 27.43F + 10.64FR + 1.85FVP + 11.79I - 26.1W + 83.37T$						6.12	158.57	0.495
Ln COMP. MODULUS (PSI)	$\ln y_2 = 38.1 - 0.73C + 23.59M - 0.12F + 0.319FR + 0.26FVP - 0.04I - 0.393W + 0.549T$						26.02	0.6257	0.806
FAILURE STRAIN (%)	$y_4 = 2.75 + 7.1C + 1.568M - 1.3F - 1.15FR - 7.86FVP + 0.16I + 5.93W - 4.07T$						55.64	3.93	0.899
TEST OF HYPOTHESES	***α = 5%***	***N = 59***	***k = 8***	***v = N-1-k = 50***	***$v_1 = k = 8$ $v_2 = N-1-k = 50$***		***$t_\alpha = 1.676$ $F_\alpha = 2.13$***		
IMPROVED MODEL EQUATIONS AND STATISTICS FROM SAS PROGRAMS							***F***	***s***	***R²***
MAX. COMP. STRESS (MPa)	$y_1 = 963.15 + 682.8M - 2.21F + 1.16FR + 2.66T$						80.52	4.17	0.856
Ln COMP. MODULUS (MPa)	$\ln y_2 = 37.9 - 0.76C + 23.45M + 0.31FR + 0.26FVP + 0.53T$						41.9	0.62	0.798
FAILURE STRAIN (%)	$y_4 = 1.63 + 7.01C - 1.27FR - 7.86FVP + 6.72W - 4.31T$						85.86	3.98	0.890
TEST OF HYPOTHESES	***α = 5%***	***N = 59***	***k = 5***	***v = N-1-k = 53***	***$v_1 = k = 5$ $v_2 = N-1-k = 53$***		***$t_\alpha = 1.674$ $F_\alpha = 2.389$***		
MODEL EQUATIONS AND STATISTICS AFTER ELIMINATION OF OUTLIERS							***F***	***s***	***R²***
MAX. COMP. STRESS (MPa)	$y_1 = 975 + 691.47M - 2.1F + 1.17FR + 2.24T$						104.49	3.58	0.899
Ln COMP. MODULUS (MPa)	$\ln y_2 = 33.4 - 0.67C + 20.25M + 0.35FR + 0.26FVP + 0.4T$						47.29	0.53	0.837
FAILURE STRAIN (%)	$y_4 = 1.62 + 6.64C - 1.46FR - 7.86FVP + 7.151W - 3.81T$						133.83	3.04	0.936
TEST OF HYPOTHESES	***α = 5%***	***N = 52***	***k = 5***	***v = N-1-k = 46***	***$v_1 = k = 5$ $v_2 = N-1-k = 46$***		***$t_\alpha = 1.679$ $F_\alpha = 2.428$***		

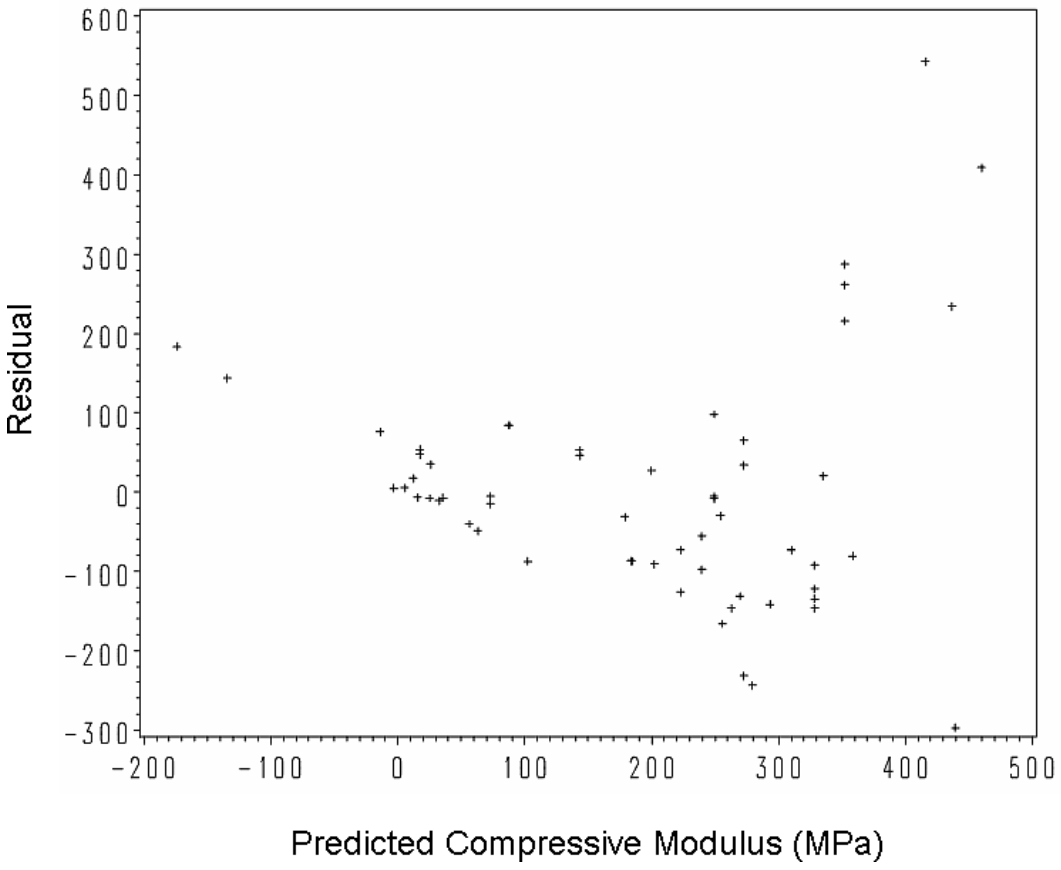

Figure 4. Residuals plot for compressive modulus

The compressive modulus model had very good results as well. Twelve data points were outside the $y_i^P \pm s$ boundary while most data points were enclosed by an $y_i^P \pm 1.5s$ interval. In contrast to the linear model, the logarithmic model didn't result in negative values thus making physical sense. Further manipulation of the data didn't bring any noticeable improvements. The conclusions from this model fitting are the following:

(1) Decreasing the amount of aluminum cation increased the compressive failure strain of the samples while reducing the compressive modulus. Cation amount was not a significant factor for the maximum compressive stress.

(2) N,N'-Methylenebisacrylamide imparted samples with higher compressive stress and compressive modulus without an appreciable effect on compressive failure strain. Comonomer also significantly raised the tensile strength.

(3) The ratio of hausmannite to fly ash affected all dependent variables: increasing it resulted in higher maximum compressive stress, lower failure strain and higher compressive modulus. Below a filler ratio of 0.5 vol. Hausmannite / vol. fly ash the samples do not harden. For economic reasons it is desired to use as little hausmannite as possible and the effect of filler ratio on the mechanical properties is less noticeable than those of the monomer/cation ratio, time and comonomer/monomer ratio.

(4) Increasing the filler volume percentage affected the failure strain and the compressive modulus by making the cement less flexible. However, the largest effect of this variable is on the rheology of the uncured mixture.

(5) Adding glass fibers reduced the mechanical properties of the cements.

(6) Increasing initiator diminished the maximum compressive stress; with no effect on compressive failure strain and compressive modulus. Overall, the effect of initiator amount was small. The range studied did not adequately address this variable; eventually with no initiator the samples would not harden. However, this study showed that initiator amount cannot be used to improve cement properties.

(7) Increased curing time results in less flexible, higher strength samples.

CHAPTER 4

XPS AND FTIR CHARACTERIZATION

X-ray Photoelectron Spectroscopy

Figure 5 shows XPS spectra for hausmannite treated with aluminum chloride solutions at different concentrations (no organic material.) The XPS spectra for hausmannite with only water show lead and carbon. Lead is considered to be a ghost peak because it was ill-defined in shape and represents an extremely low concentration of this element[43]. The amount of carbon was also very low and assumed to be from sample handling; it is almost impossible to totally eliminate carbon in XPS spectra. The following were identified as being present at non-trace levels: manganese with binding energies corresponding to 655 eV and 643 eV for the $2p_{1/2}$ and $2p_{3/2}$ levels, and 89 eV and 50 eV to the 3s and 3p levels and oxygen with binding energies of 531 eV for the 1s level and 29 eV for the 2s level. These binding energies lead to the identification of this compound as Mn_3O_4, which agrees with the literature[44]. Table 15 shows the concentration table for all spectra compensated for carbon and lead, i.e. carbon and lead peaks were not included in the calculation.

Table 15. Atomic concentrations on aluminum chloride treated hausmannite

[$AlCl_3$] M	**O 1s**	**Al 2p**	**Cl 2p**	**Mn $2p_3$**
0.00	65.85	-	-	34.15
0.25	68.81	1.38	11.50	18.31
0.50	69.92	3.05	9.14	17.89
0.75	64.10	5.91	13.10	16.86

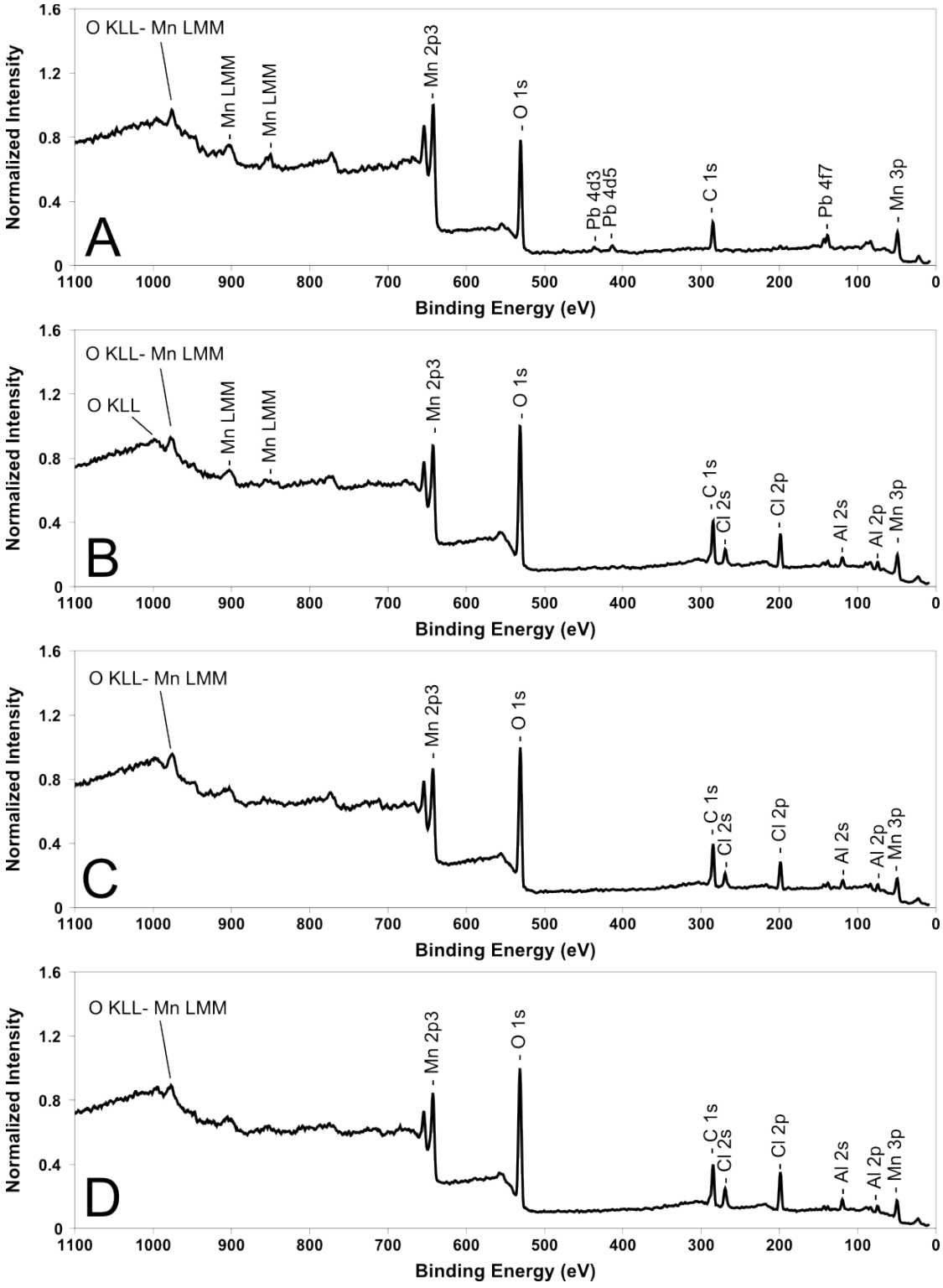

Figure 5. XPS spectra for hausmannite equilibrated with aluminum chloride at different concentrations. A) [$AlCl_3$] = 0 M, B) [$AlCl_3$] = 0.25 M, C) [$AlCl_3$] = 0.50 M, D) [$AlCl_3$] = 0.75 M

When the concentration of aluminum chloride is increased to 0.25 M, new lines are detected for aluminum and chlorine. Of particular importance are the lines at 74.3 eV for aluminum and 203 eV for chlorine. These results are similar to those of the catalyst $MnO/\gamma\text{-}Al_2O_3$ XPS spectra found in the literature[45] prepared by thermally decomposing a $Mn(OH)_2$ and $Al(OH)_3$ synthesized from the hydrolysis of $Al(NO_3)_3$ and $Mn(NO_3)_2$. In this catalyst however, Al_2O_3 was present in a much larger amount than MnO. Figure 6 shows the peaks for Al 2s, Cl 2s, Mn $2p_3$, and O 1s. The line for aluminum at 74.3 eV can be assigned to the bond Al-O and the line at 203 eV to the bond Mn-Cl. Further evidence is supplied by the splitting of the oxygen peaks at 530 eV and 532 eV which can be assigned to the bonds Al-O and Mn-O. Also, one of the peaks for Mn is displaced to 642 eV which corresponds to Mn-Cl. As the aluminum chloride concentration increases, the aluminum and chlorine peaks intensify while the manganese peaks lose intensity. In other words, a non-cement forming filler (Mn_3O_4) is coated with a material suitable for cement formation.

Figure 7 shows the spectra for hausmannite treated with poly(acrylic acid) and acrylic acid with and without aluminum chloride. From the atomic concentration data shown on Tables 16 and 17 it can be seen that the surface of the filler has been covered almost completely with carbon and oxygen. Figure 8 shows XPS spectra and Table 5 the calculated atomic concentrations for hardened polyalkenoate cements based on hausmannite using formulations given in Table 5, which are very similar to the formulations with PAA shown in Figure 7. The additional peaks due to calcium and silicon in two of the formulations come from the inert flyash filler. Despite the fact that large amounts of aluminum chloride were added, no aluminum peaks are detected which leads us to conclude that significant amounts of aluminum cation have been adsorbed on

the surface of the hausmannite. These samples are pulverized cement, and the surface is expected to be primarily polymer if the polymer-filler interface is stronger than the cohesive strength of the polymer. The high level of carbon indicates that our supposition was correct, the surface is primarily polymer. As further proof, using this level of carbon to calculate the oxygen percentage that should be present indicates that greater than 90% of the oxygen in the XPS spectra comes from polymer. Hence, the fact that aluminum is not detected by XPS indicates that aluminum is adsorbed by the hausmannite and a polymer layer is covering the filler.

Table 16. Atomic concentrations from XPS on the surface of hausmannite

[PAA] M	[AA] M	[$AlCl_3$] M	C 1s	O 1s	Al 2p	Cl 2p	Mn $2p_3$
-	4,4	-	52.85	40.24	-	-	6.94
-	4.4	0.5	54.61	36.5	0.00	3.04	5.85
0.08	-	-	62.07	36.95	-	-	0.98
0.08	-	0.5	57.43	37.5	3.15	1.92	-

Table 17. Atomic concentrations from XPS on the surface of hausmannite based polyalkenoate cement formulations in Table 5

Formulation	C 1s	O 1s	Al 2p	Cl 2p	Mn 2 p_3
1	59.18	34.06	-	2.36	4.04
2	61.63	35.33	-	-	3.04
3	57.23	33.07	0.00	7.76	-
4	51.84	42.28	1.4	1.13	-

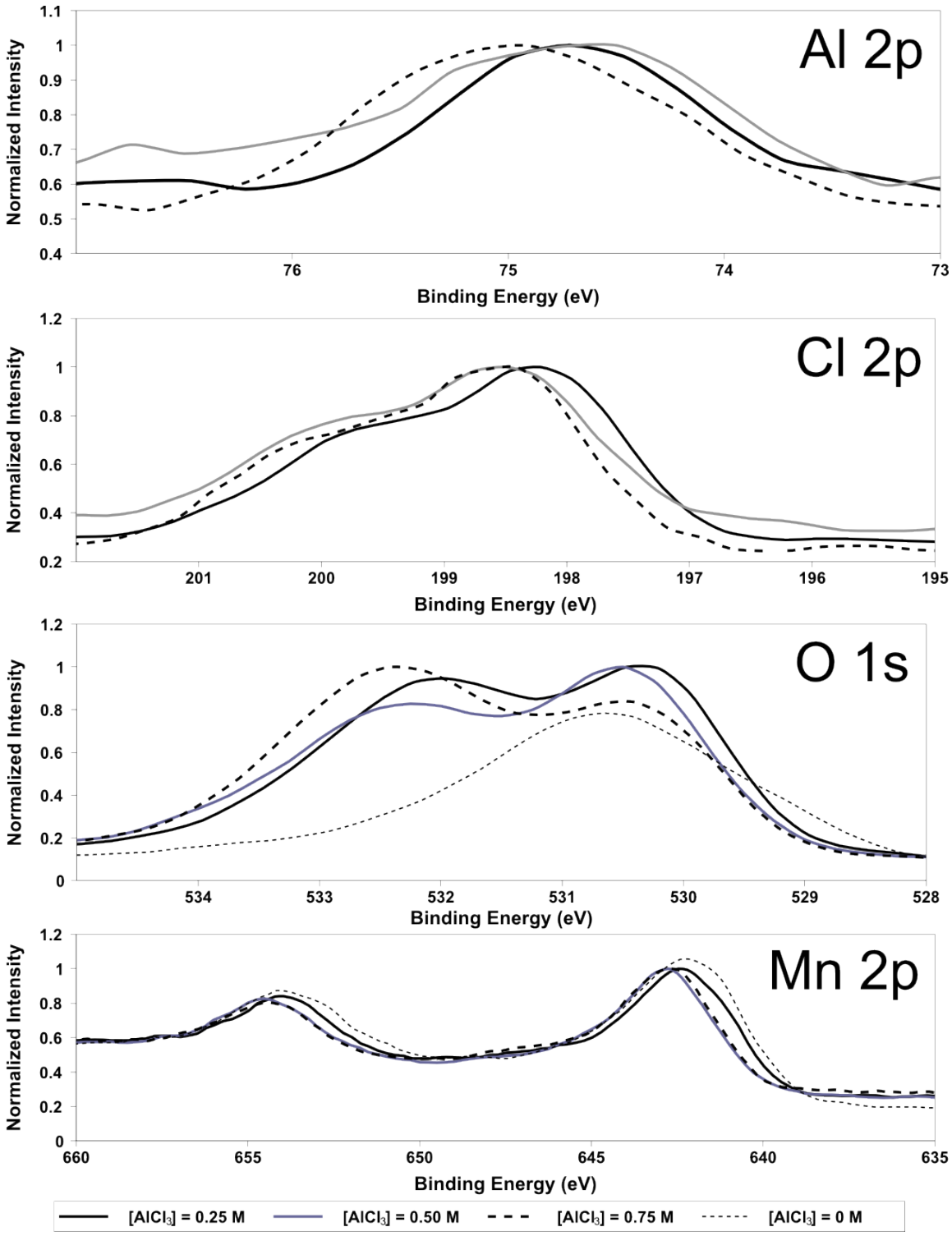

Figure 6. XPS spectra for regions corresponding to Al 2p, Cl 2p, O 1s and Mn 2p

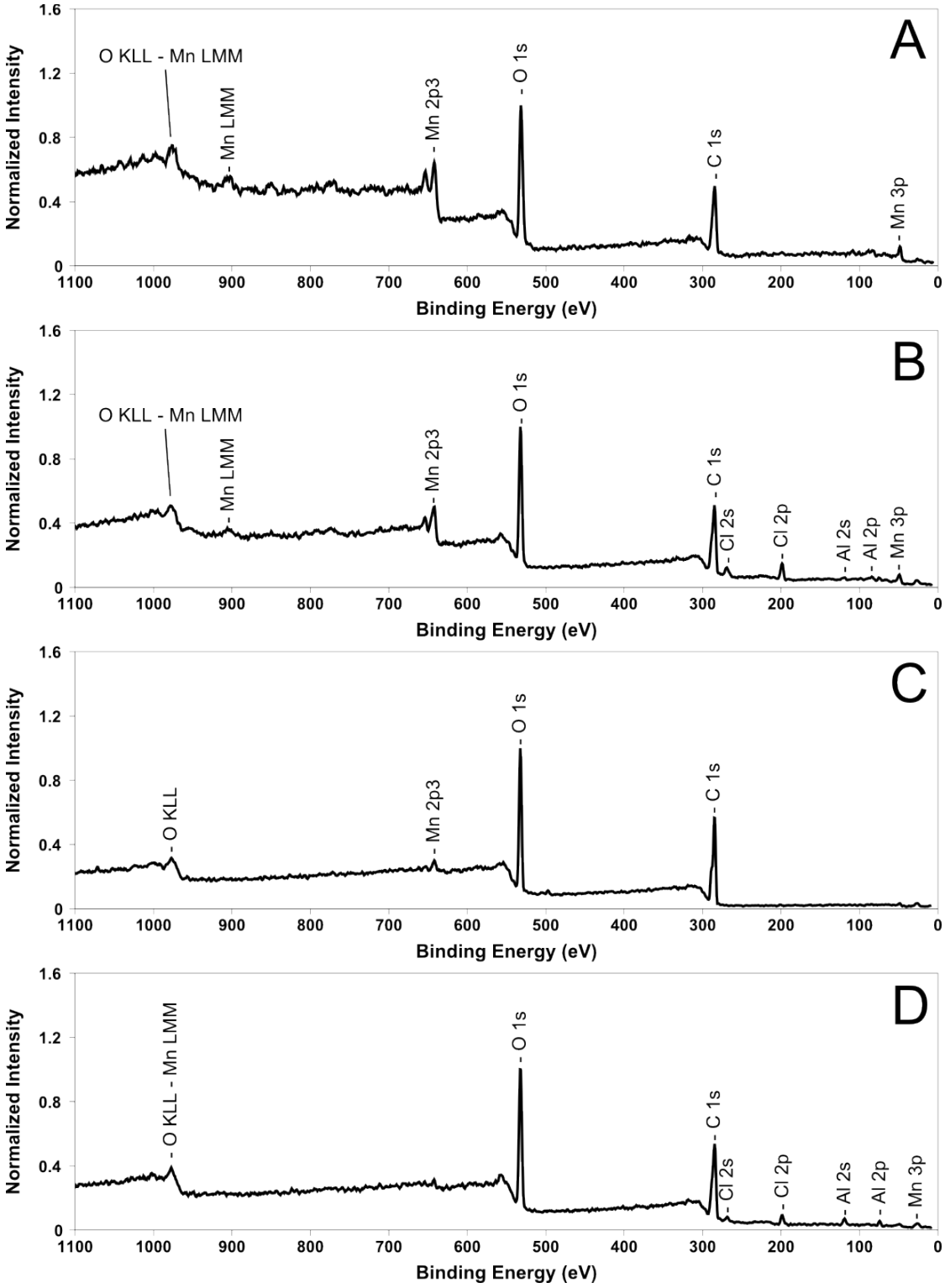

Figure 7. XPS spectra of centrifuged samples. A) hausmannite + acrylic acid, B) hausmannite + acrylic acid + aluminum chloride, C) hausmannite + poly(acrylic acid), D) hausmannite + poly(acrylic acid) + aluminum chloride

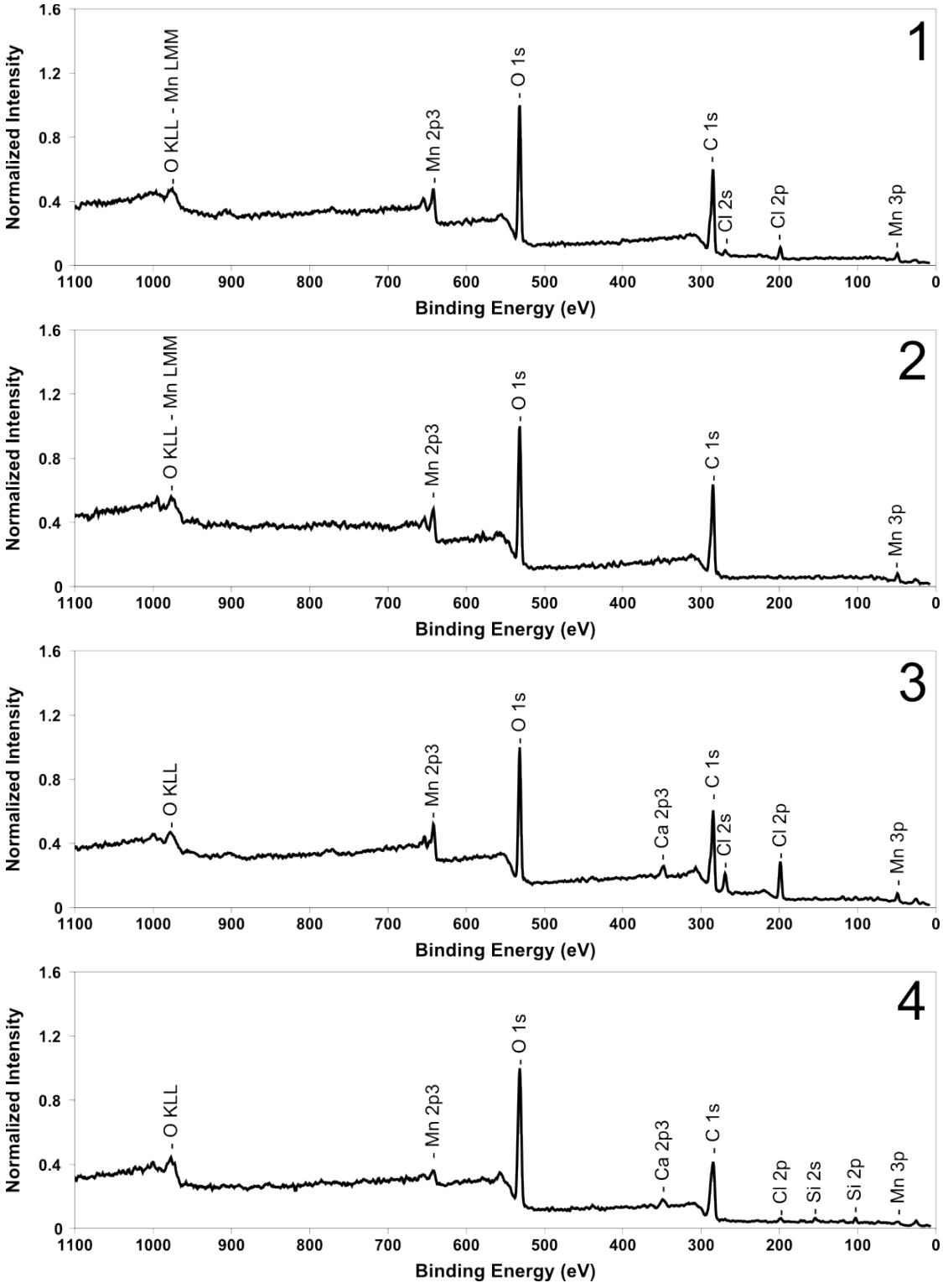

Figure 8. XPS spectra for polyalkenoate cement based on hausmannite—formulations in Table 5

Fourier Transfrom Infrared Spectroscopy

The molecular structure of polyalkenoate cements has been investigated using infrared spectroscopy. The bonds between PAA and Na^{+}, Mg^{2+}, Ca^{2+} are purely ionic, but absorbance bands of other cation-PAA interactions (e.g., Zn^{2+} (1540-1560 cm^{-1}), Al^{3+} (1600 cm^{-1})) show evidence of complex formation. In previous work, the strength and stability of polyalkenoate cements correlated with the complexation constants of the cations[2]. In order to assign correctly the absorbance bands it is necessary to verify for interference due to occluded water and the hausmannite filler in the polyalkenoate cements. Water ,for instance, has two peaks at approximately 3500 cm^{-1} and 1600 cm^{-1}. Also, to verify that the base line was not affected by hausmannite, a blank sample of hausmannite in KBr was prepared and measured by FTIR. This sample presented peaks at 420 cm^{-1}, 530 cm^{-1} and 640 cm^{-1} in agreement with the literature[46, 47]. Other than these peaks at 3400 cm^{-1}, 1600 cm^{-1}, 640 cm^{-1}, 530 cm^{-1} and 420 cm^{-1}, the remaining peaks are deemed to be due to carboxylic acids or coordination with either Mn^{2+} or Al^{3+}. Figure 9 shows the FTIR spectra of the hausmannite mixed with acrylic acid and poly(acrylic acid) with and without aluminum chloride. Figure 10 shows polyalkenoate cement formulations' FTIR spectra from Table 5. Each spectrum has a set of peaks corresponding to specific vibrational states of the molecules. The relevant peaks are: 1700 cm^{-1} (υC=O dimer form of carboxylic acids.), 1600~1550 cm^{-1} (antisymmetric stretching of carboxylate; indicates the presence of an inorganic salt of a carboxylic acid.), 1400~1450 cm^{-1} (symmetric stretching of carboxylate indicating the presence of an inorganic salt of a carboxylic acid.), 1000~1300 cm^{-1} (carboxylic acid.). When an acid is converted into its inorganic salt, the characteristic frequencies 1420 cm^{-1}, 1000~1300 cm^{-}

[1], and 920 cm^{-1} are replaced by 1600~1550 cm^{-1} and 1400~1450 cm^{-1} pair of characteristic frequencies[48]. In the majority of the cement formulations and dried solids from the centrifuged samples, these latter bands are present leading us to conclude that metal-carboxylate coordination occurs. All of the samples appear to contain some water, as indicated by absorbances at 3450 cm^{-1} and 1650 cm^{-1}, which overlaps with the 1550-1600 cm^{-1} carboxylate salt absorbance. However, relative intensities of the carboxylic acid carbonyl peak (1700 cm^{-1}) and its carboxylate peak (1400-1450 cm^{-1}) peak can be used to make qualitative comparisons of the degree of metal complexation among the different samples.

Dried Solids from Centrifuged Samples

AA + Hausmannite

Because no aluminum chloride was added to this sample, the peak at 1450 cm-1 is due to manganese carboxylate complex formation[49, 50]. A significant fraction of acid exists in the sample as evidenced by the 1700 cm^{-1} peak. Peaks in the 400-1000 cm^{-1} region result from hausmannite.

AA + Hausmannite + Aluminum chloride

The 1450 cm^{-1} peak, which is asymmetric as compared to the peak with only manganese present, can be assigned to coordination with both manganese and aluminum. The degree of metal complexation appears to be greater than in the previous sample without aluminum chloride, based on the ratio of the 1700 cm^{-1} and 1450 cm^{-1} peak intensities.

PAA + Hausmannite

This IR spectrum is very similar to that of the AA + Hausmannite sample. Manganese coordination (1450 cm^{-1}) and carboxylic acid (1700 cm^{-1}) are present in approximately the same ratios.

PAA + Hausmannite + Aluminum chloride

PAA-metal cation coordination (both manganese and aluminum) is evident based on the 1450 cm^{-1} peak as with the AA + Hausmannite + $AlCl_3$ sample. This sample is representative of polyalkenoate cements based on hausmannite although the formulation did not harden because of the high water content from the poly(acrylic acid) (i.e., 51% water), and the cation source solution (i.e., 74% water). However, after centrifuging the sample, removing the liquids and drying, the solid mass was hard and homogeneous.

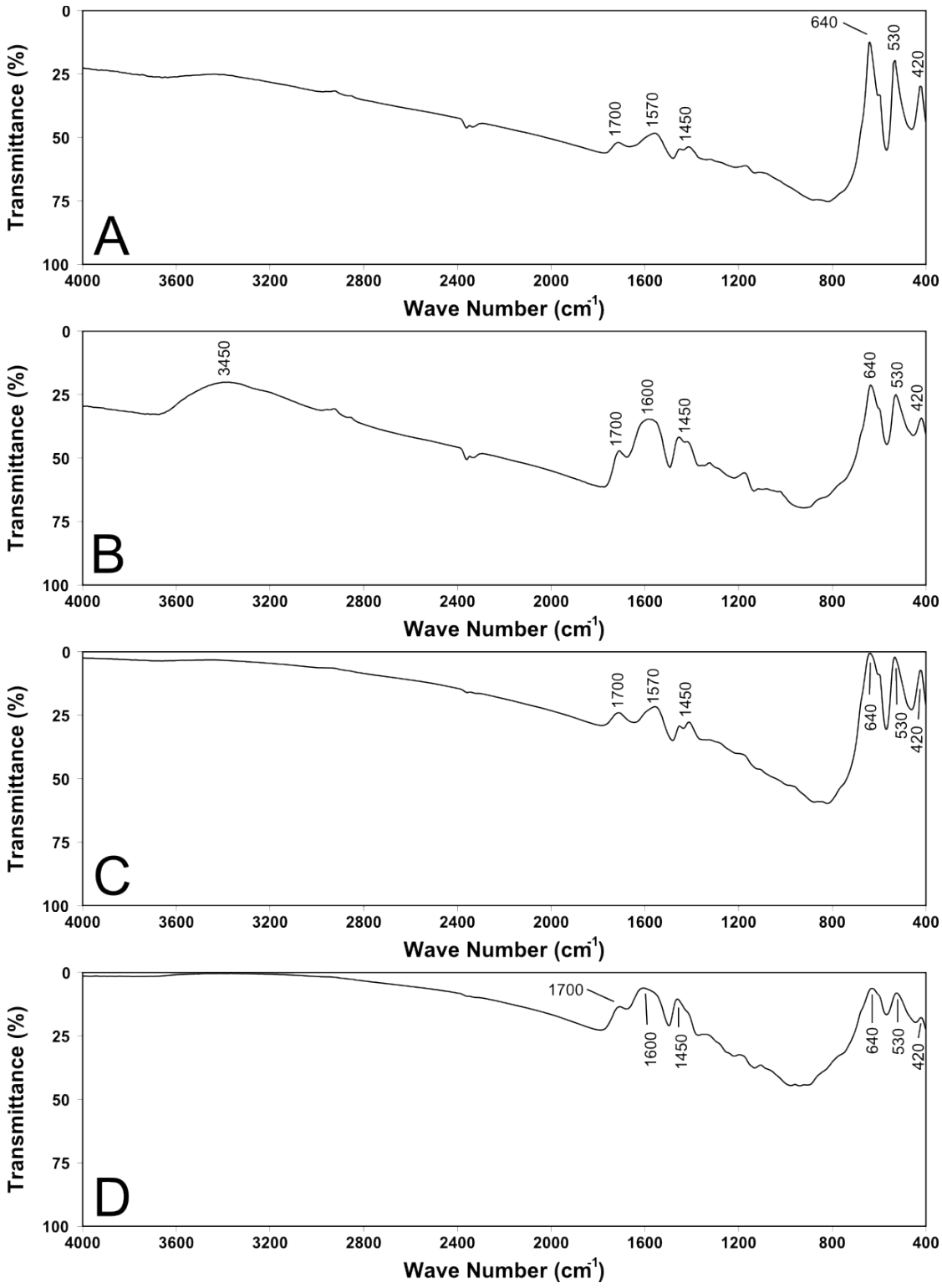

Figure 9. FTIR spectra of hausmannite reacted with acrylic and poly(acrylic acid). A) hausmannite + acrylic acid, B) hausmannite + acrylic acid + aluminum chloride, C) hausmannite + poly(acrylic acid), D) hausmannite + poly(acrylic acid) + aluminum chloride

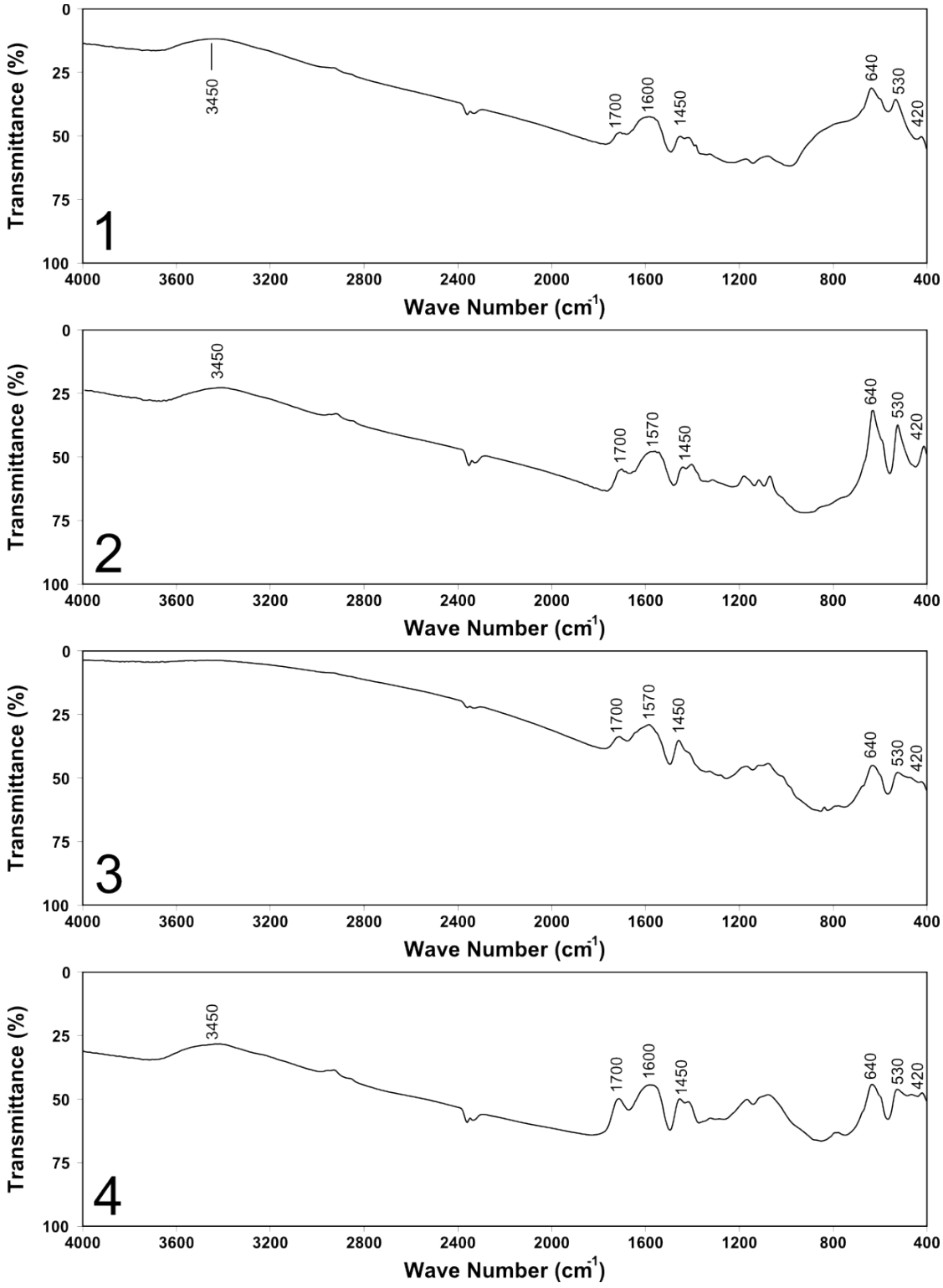

Figure 10. FTIR spectra of polyalkenoate cement based on hausmannite—formulations in Table 5

Cements

IR spectra for the cements are very similar (Figure 6). The most obvious differences are in the 400-1000 cm^{-1} range. In formulations 3 and 4, which contain flyash, the peak at 420 cm^{-1} is overlapped by a neighboring peak at ~460 cm^{-1}. This peak is probably due to Fe_2O_3 present in the flyash filler[51]. However, the slight differences in the peaks at 1450 cm^{-1} can be correlated to mechanical properties shown in Table 6. In polyalkenoate cements, higher crosslinking density results in higher compressive strength and higher modulus. The two samples containing fly ash have higher compressive strength, indicating a higher degree of crosslinking than in the corresponding cements with hausmannite-only filler. Based on the results from the centrifuged samples, aluminum complexation increases the 1450 cm^{-1} absorbance. The hausmannite-only filler cements (spectra 1 and 2), have proportionately smaller 1450 cm^{-1} peaks than the cements containing a mixture of hausmannite and fly ash (spectra 3 and 4). A lower level of crosslinking in the hausmannite-only filler cements is consistent with excessive aluminum hydrolysis caused by the basic hausmannite surface. Of course, some neutralization is necessary in order to partially deprotonate the polyacid so complexation can occur. By diluting the hausmannite with fly ash, more favorable conditions for aluminum crosslinking are obtained.

Mn^{2+} and Al^{3+} have been shown to have a coordination number of 6 in aqueous environments[50]. Several hypothetical molecular structures have been proposed for polyalkenoate cements based on FTIR spectra. In general these cations (Mn^{2+} and Al^{3+}) can coordinate with multiple polyalkenoate strands and any remnant charges be balanced by either Cl^- or OH^- groups. Some possibilities for coordination with a single polymer

strand are shown in Figure 11. Of these, the structures on Figure 11A and 11B are the most likely to happen due to less steric hindrance. The remaining structures on Figure 11 require bending of the polyalkenoate chain (Figures 11C and 11D) or strain in the chelate at the carboxyl group, where the charge is distributed, bonded with either Mn^{2+} or Al^{3+} (Figures 11E and 11F). When the cations Mn^{2+} or Al^{3+} are coordinating with two polymer chains, many more configurations are possible. However, considering that Mn-Cl bonds were shown in the XPS analyses, it is unlikely to have Mn^{2+} coordinating with two polyalkenoate strands as shown in Figure 12A and 12C. Some configurations with Al^{3+} are offered. As it can be seen in Figure 12B, the polymer strands are already perpendicular to each other leading us to believe that steric hindrance limits the way polyalkenoate strands can be accommodated. Figure 12D shows a chelated structure with two polymer strands for Al^{3+} that also has the tension at the carboxylate group aforementioned. Other theoretical structures with three or more carboxylates interacting with Al^{3+} are deemed unlikely due to steric hindrance[55].

Table 18. Mechanical properties of polyalkenoate cements using compositions given in Table 5

RUN	***C***	***FR***	***Max. Comp. Strength (PSI)***	***Comp. Modulus (PSI)***	***Fail Strain (%)***
1	10	0	258	5333	8.75
2	40	0	842	5000	22.5
3	10	1	1766	67000	4
4	40	1	1071	5684	21.5
VARIABLES				***DEFINITION***	
CATION RATIO (C)				mol Acrylic Acid / mol Cation	
FILLER TYPE RATIO (FR)				vol. Hausmannite / vol. flyash	

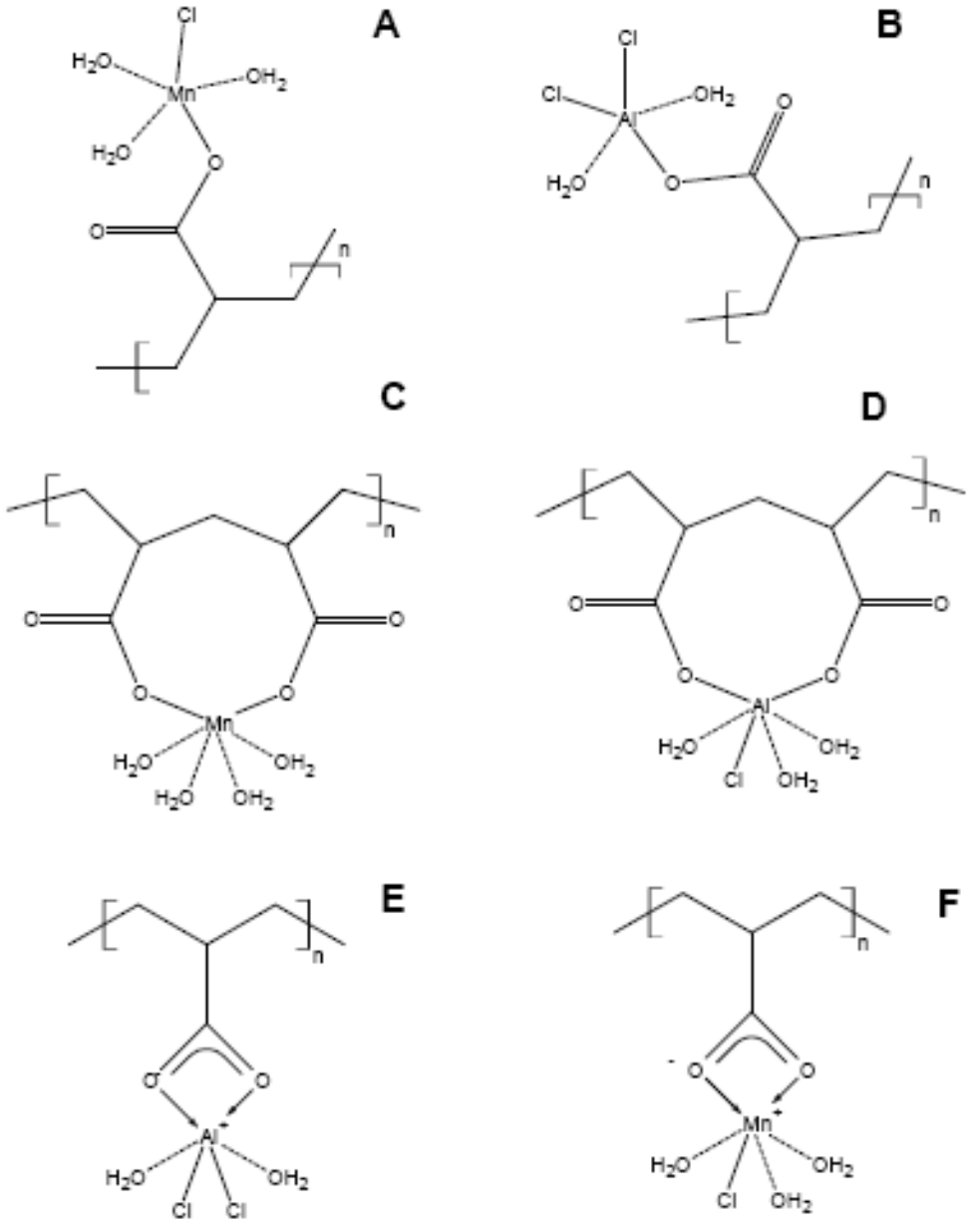

Figure 11. Schematics of possible structures for Mn^{2+} and Al^{3+} in polyalkenoate cement based on hausmannite neutralized by Cl^- with one polyalkenoate polymer strand

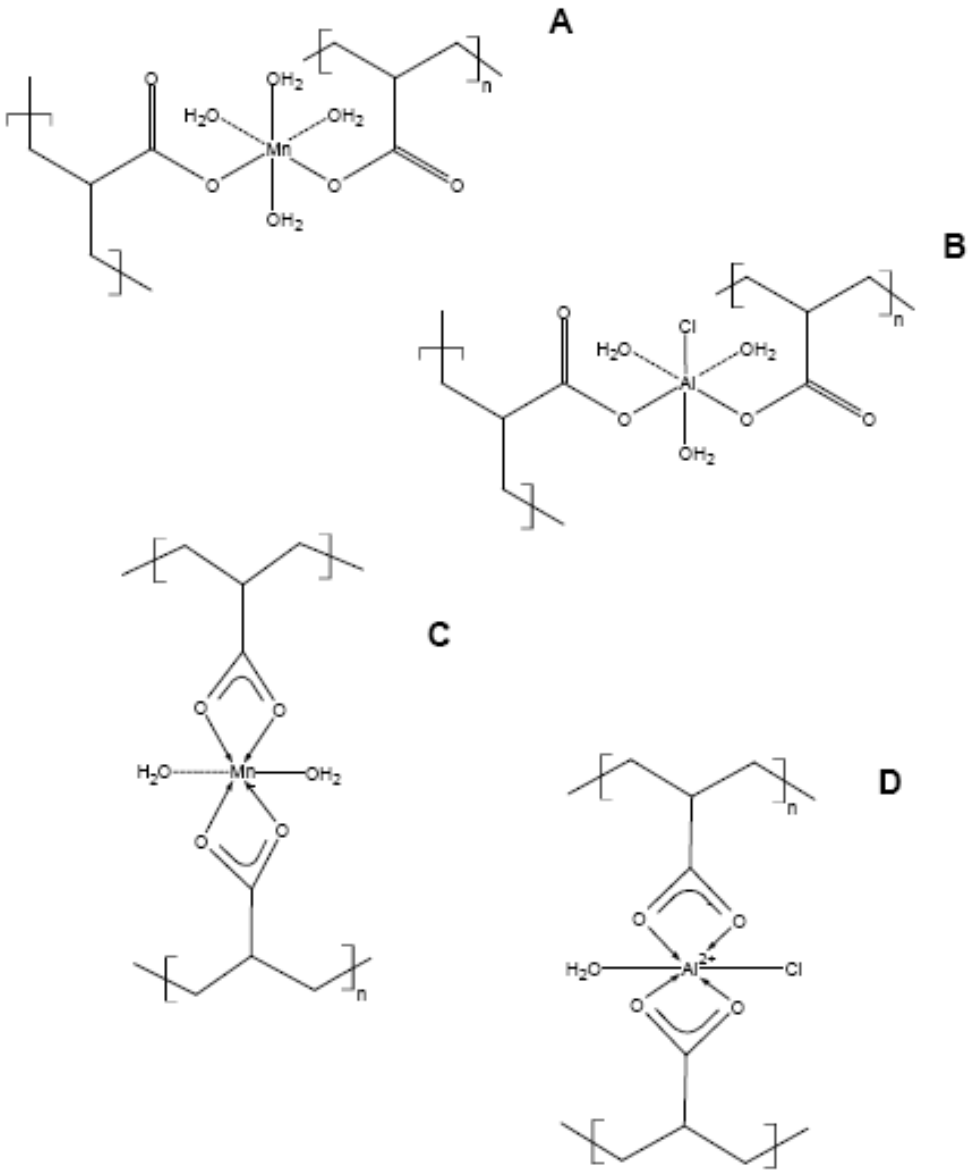

Figure 12. Schematics of possible structures for Mn^{2+} and Al^{3+} in polyalkenoate cement based on hausmannite neutralized by Cl^- with two polyalkenoate polymer strands

CHAPTER 5

CONCLUSIONS AND RECOMMENDATIONS

Conclusions

Design of experiments proved to be an excellent way to develop polyalkenoate cement formulations that harden by a combination of free radical polymerization and multivalent cation crosslinking. The independent variables selected for the design of experiments were bound by physical and economical constraints. The first step was to determine approximate operating ranges: among low-cost fillers non-hausmannite containing formulations didn't harden, formulations with a monomer/water ratio below 0.8 vol. acrylic acid/vol. water didn't harden, formulations with a monomer/cation ratio above 80 mole acrylic acid/mole inorganic cation source didn't harden and at 35% by volume solids the slurries had rheological characteristics that prevented measurement by the equipment used to characterize the rheology of cements.

The mechanical properties of the cement were highly affected by hardening time, amount of aluminum cation and N,N'-methylenebisacrylamide/acrylic acid (comonomer) mole ratio. Longer curing times and more cation resulted in less flexible, higher strength samples. Higher comonomer/monomer ratios resulted in higher strength samples with little or no change in flexibility. All other variables had an insignificant effect on the mechanical properties. One variable not studied with a large range was monomer/water ratio. Since the economic penalty for changing this variable was high, we found a minimum monomer/water volume ratio that consistently led to hardened samples and fixed this parameter. In the final multivariable analysis of compressive properties, no

interactions were needed; while the only interaction needed for the tensile strength was the interaction between the organic and ionic crosslinker.

It is possible to produce hausmannite based polyalkenoate cements by free radical polymerization of acrylic acid in presence of hausmannite and aluminum chloride. Aluminum and manganese from hausmannite cations coordinate with the carboxylic acids. Aluminum chloride in solution covering hausmannite results in a low pH slurry that allows Mn^{2+} cations to coordinate with carboxylic acids. Cation crosslinking and remnant carboxylic acids were correlated with the mechanical properties and the FTIR spectra. It was found that higher crosslinking by Al^{3+} and low contents of residual carboxylic acids resulted in stronger cement formulations. This result was obtained by augmenting the amount of $AlCl_3$ in the formulations or by the inclusion of flyash in the formulations that essentially diluted the hausmannite filler leading to less coordination by Mn^{2+} with carboxylic acids. Nonetheless, hausmannite is still necessary in the formulations for cement hardening because it causes the pH of the slurry to augment leading to the deprotonation of polyalkenoic and carboxylic acids in solution facilitating their corrdination with Al^{3+}.

Recommendations

As far as devicing a material capable of fulfilling certain needs at a reasonable cost, this project is done. However, as far as the ideas that can be used to further investigate around this topic there are a lot. For instance, the possibility of ions migration was questioned at the beginning of this project and no answer could be given based on the existing data at that time. Nonetheless, this has been investigated for many other polyalkenoate cements and the process is rather simple: submerge a sample of

polyalkenoate cement in water (or oil) and then measure the water (or oil) for manganese or any other relevant cations and carbon. Also, dry out the sample and by weight comparison see if there was any weight loss or gain after a given time. The use of polyalkenoate materials to deliver drugs has been discussed[2] and this indicates that there is also a need to see how any mass transport phenomena leading degradation is occurring in manganese tetraoxide based polyalkenoate cements and how to avoid it. Which leads to another idea: porosity measurements on manganese tetraoxide polyalkenoate cements. In short, this material ought to be characterized more by taking the same measurements that have been done with Portland cements.

One of the most important properties of cement slurries is the setting time. This is because cement slurries need to be pumped before any hardening occurs. Unfortunately, the setting times obtained for the materials in this project were rather low (approximately 30-35 minutes). Several ideas can be considered to remedy the situation: it has been postulated that the amount of aluminum influences setting time and that if it is readily available the setting reaction is augmented. One way to counteract this is by using chelated aluminum instead of aluminum chloride. Other possibility is to include a competing agent such as tartaric acid to make a complex of aluminum in the formulation and slow down the setting process[3, 5]. Of course, the idea of studying the setting time alone and ways to increase it, is only a minor part of the rheological charaterization of reacting slurries such as one of the many studies already available in literature[56-]. Nonetheless, the topic of polyalkenoate cements rheology needs to be studied further by performing viscosity measurements while the setting reaction is progressing and seeing how the rheology is affected by chelating agents and cation sources delivered in the form of chelates.

REFERENCES

(1) Smith, D.K. *"Cementing"*, H.L. Doherty Memorial Fund of AIME, Society of Petroleum Engineers, New York, NY, 1990

(2) Wilson, A.D.; Nicholson, J.W. *Acid-base Cements--Their Biomedical and Industrial Applications*, Cambridge University Press, Cambridge, Great Britain, 1993

(3) Culbertson, B.M. *Prog. Polym. Sci.*, **2001**, *26*, 577

(4) Kenny, S.M.; Buggy, M. *J. Mater. Sci.: Mater. Med.*, **2003**, *14*, 923

(5) Wilson, A.D.; Hill, R.G.; Warrens, C.P.; Lewis, B.G. *J. Dent. Res.*, **1989**, *68*, 89

(6) Braybrook, J.H.; Nicholson, J.W. *J. Mater. Chem.*, **1993**, *3*, 361

(7) Asmussen, E.; Peutzfeldt, A. *Dent. Mater.*, **2003**, *19*, 620

(8) Kenny, S.; Hill, R.G.; Towler, M. *J. Mater. Sci.: Mater. Med.*, **2000**, *11*, 847

(9) Towler, M.R.; Crowley, C.M.; Murphy, D.; O'Callaghan, A.M.C. *J. Mater. Sci. Lett.*, **2002**, *21*, 1123

(10) Sullivan, A.; Hill, R. *J. Mater. Sci.*, **2000**, *35*, 1125

(11) Vargas, G.; Rivera, H.; Lopez, J.; Mendez, J.; Mendez, M.; Romero, J. *Bol. Soc. Esp. Ceram.*, **2002**, *42*, 405

(12) Fennell, B.; Hill, R.G. *J. Mater. Sci.*, **2001**, *36*, 5193

(13) Fennell, B.; Hill, R.G. *J. Mater. Sci.*, **2001**, *36*, 5177

(14) Fennell, B.; Hill, R.G. *J. Mater. Sci.*, **2001**, *36*, 5185

(15) Fong, H. *J. Appl. Polymer Sci.*, **2004**, *94*, 492

(16) Magi, J.; Jincy, J.; Beena, M. *J. Macromol. Sci. Pur.*, **2004**, *A41*, 85

(17) Rodriguez, E.; Katime, I. *Macromol. Mater. Eng.*, **2003**, *288*, 607

(18) Hernandez, R.; Lopez, D.; Perez, E.; Mijangos, C. *Macromol. Symp.*, **2005**, *222*,

163

(19) Cook, W.D. *J. Biomed. Mater. Res.*, **1983**, *17*, 1015

(20) Sullivan, A.; Hill, R.G.; Waters, K. *J. Mater. Sci. Lett.*, **2000**, *19*, 325

(21) Hodd, K.A.; Reader, A.L. *Brit. Polym. J.*, **1976**, *8*, 131

(22) Kleverlaan, C.J.; Van Duinen, R.N.B.; Feilzer, A.J. *Dent. Mater.*, **2004**, *20*, 45

(23) Yatsimirksii, K.B.; Vasil'ev, V.P. *Instability Constants of Complex Compounds*, Pergamon, Elmsford, NY, 1960

(24) Wells, C.F.; Davies, G. *Nature*, **1965**, *205*, 692

(25) Hornsby, P.R.; Merson, S.A.; Prosser, H.J.; Wilson, A.D. *J. Mater. Sci.*, **1982**, *17*, 3575

(26) Nicholson, J.W. *J. Appl. Polym. Sci.*, **1998**, *70*, 2353

(27) Cavell, E.A.S.; Gilson, I.T. *J. Polym. Sci. A1*, **1966**, *4*, 541

(28) Crisp, S.; Merson, S.A.; Wilson, A.D. *Ind. Eng. Chem. Prod. Res. Dev.*, **1980**, *19*, 403

(29) Kemmitt, T.; Mills, A.M.; Graeme, J.G. *Aust. J. Chem.*, **2001**, *54*, 37

(30) Kung, K.H.; McBride, M.B. *Clays Clay Miner.*, **1988**, *36*, 297

(31) Murray, J.W.; Dillard, J.G.; Giovanoli, R.; Moers, H.; Stumm, W. *Geochim. Cosmochim. Acta*, **1985**, *49*, 463

(32) Kinniburgh, D.G.; Cooper, D.M. *Environ. Sci. Technol.*, **2004**, *38*, 3641

(33) Shaughnessy, D.A.; Nitsche, H.; Booth, C.H.; Skuh, D.K.; Waychunas, G.A.; Wilson, R.E.; Gill, H.; Cantrell, K.J.; Serne, R.J. *Journal: Environ. Sci. Technol.* **2003**, 37, 3367

(34) Rocak, D.; Kosec, M.; Degen, A. *J. Eur. Ceram. Soc.*, **2002**, *22*, 391

(35) Srinivasan, C.B.; Narasimhan, N.; Lakshmi, N.; Ilango, S.V. *Cement Concr. Res.*,

2003, *33*, 1287

(36) Box, G.E.P.; Hunter, J.S.; Hunter, W.G. *Statistics for Experimenters, An Introduction to Design, Data Analaysis and Model Building*, John Wiley and Sons. Ltd., Hoboken, NJ, 1978

(37) Nishibayashi, S.; Yoshino, A. *Superplasticizers and Other Chemical Admixtures in Concrete SP-173*, American Concrete Institute, Farmington Hills, MI, 1997

(38) Usui, H.; Li, L.; Kinoshita, S.; Suzuki, H. *J. Chem. Eng. Jpn.*, **2001**, *34*, 360

(39) Park, H.C.; Yoon, S.Y.; Lee, Y.B.; Kim, B.K.; Stevens, R. *J. Mater. Synth. Process.*, **2002**, *10*, 237

(40) Mitchell, C.A.; Douglas, W.H.; Cheng, Y.S. *Dent. Mater.*, **1999**, *15*, 7

(41) Mitsihashi, A.; Hanaoka, K.; Teranaka, T. *Dent. Mater.*, **2003**, *19*, 747

(42) McCabe, J.F. *Biomaterials*, **1998**, *19*, 521

(43) Wagner, C.; Riggs,W.; Davis, L.; Moulder, J. *Handbook of X-ray Photoelectron Spectroscopy*, Perkin Elmer Corporation, Eden Prairie, MN, 1979

(44) Audi, A.A.; Sherwood, P.M.A. *Surf. Interface Anal.*, **2002**, *33*, 274

(45) Xu, H.L.; Shen, W.; Yang, Y.T. *Chinese J. of Chem.*, **2001**, *19*, 647

(46) Wang, W.; Xu, C.; Wang, G.; Liu, Y.; Zheng, C. *Adv. Mater.*, **2002**, *14*, 837

(47) Al Sagheer, F.A.; Hasan, M.A.; Pasupulety, L.; Zaki, M.I. *J. Mater. Sci. Lett.*, **1999**, *18*, 209

(48) Nakanishi, K.; Solomon, P.H. *Infrared Spectroscopy*, Holden Day, San Francisco, CA, 1977

(49) Matzapetakis, M.; Karligiano, N.; Bino, A.; Dakanali, M.; Raptopoulou, C.P.; Tangoulis, V.; Terzis, A.; Giapintzakis, J.; Salifoglou, A. *Inorg. Chem.*, **2000**, *39*, 4044

(50) Lide, D.R *CRC Handbook of Chemistry and Physics*, CRC Press, Boca Raton, FL,

1992-1993

(51) Willis, A.L.; Turro, N.J.; O'Brien, S. *Chem. Mater.*, **2005**, *17*, 5970

(52) Lee, W.K.W.; van Deventer, J.S.J. *Langmuir*, **2003**, *19*, 8726

(53) Fermo, P.; Cariati, F.; Pozzi, A.; Demartin, F.; Tettamanti, M.; Collina, E.; Lasagni, M.; Pitea, D.; Puglisi, O.; Russo, U. *Fresen. J. Anal. Chem.*, **1999**, *365*, 666

(54) Potgieter-Vermaak, S.S.; Potgieter, J.H.; Belleil, M.; DeWeerdt, F.; Van Grieken, R. *Cement Concrete Res.*, **2006**, *36*, 663

(55) Mehrotra, R.C. *Metal Carboxylates*, Academic Press, New York, NY, 1983

(56) Fricker, J.; Hirota, K., Tamiya, Y. *Aust. Dent. J.*, **1991**, *36*, 240

(57) McMichen, F.R.; Pearson, G.; Rahbaran, S.; Gulabivala, K. *Int. Endod. J.*, **2003**, *36*, 629

(58) Hill, R.G.; Wilson, A.D. *J. Dent. Res.*, **1988**, *67*, 1446